1986-12

The effects of metallized fuel composition on the combustion characteristics of solid fuel ramjets.

Karadimitris, Adonis

NAVAL POSTGRADUATE SCHOOL
Monterey, California

THESIS

THE EFFECTS OF METALLIZED FUEL
COMPOSITION
ON THE COMBUSTION CHARACTERISTICS OF
SOLID FUEL RAMJETS

by

Adonis Karadimitris

December 1986

Thesis Advisor David W. Netzer

Approved for public release; distribution is unlimited.

SECURITY CLASSIFICATION OF THIS PAGE

REPORT DOCUMENTATION PAGE

1a REPORT SECURITY CLASSIFICATION UNCLASSIFIED	1b RESTRICTIVE MARKINGS
2a SECURITY CLASSIFICATION AUTHORITY	3 DISTRIBUTION/AVAILABILITY OF REPORT Approved for public release; distribution is unlimited.
2b DECLASSIFICATION/DOWNGRADING SCHEDULE	
4 PERFORMING ORGANIZATION REPORT NUMBER(S)	5 MONITORING ORGANIZATION REPORT NUMBER(S)
6a NAME OF PERFORMING ORGANIZATION Naval Postgraduate School 6b OFFICE SYMBOL (If applicable) 67	7a NAME OF MONITORING ORGANIZATION Naval Postgraduate School
6c ADDRESS (City, State, and ZIP Code) Monterey, California 93943-5000	7b ADDRESS (City, State, and ZIP Code) Monterey, California 93943-5000
8a NAME OF FUNDING/SPONSORING ORGANIZATION 8b OFFICE SYMBOL (If applicable)	9 PROCUREMENT INSTRUMENT IDENTIFICATION NUMBER
8c ADDRESS (City, State, and ZIP Code)	10 SOURCE OF FUNDING NUMBERS PROGRAM ELEMENT NO / PROJECT NO / TASK NO / WORK UNIT ACCESSION NO

11 TITLE (Include Security Classification)
THE EFFECTS OF METALLIZED FUEL COMPOSITION ON THE COMBUSTION CHARACTERISTICS OF SOLID FUEL RAMJETS

12 PERSONAL AUTHOR(S) Karadimitris Adonis

13a TYPE OF REPORT	13b TIME COVERED	14 DATE OF REPORT (Year Month Day)	15 PAGE COUNT
Master's Thesis	FROM _____ TO _____	1986 December	79

16 SUPPLEMENTARY NOTATION

17 COSATI CODES			18 SUBJECT TERMS (Continue on reverse if necessary and identify by block number)
FIELD	GROUP	SUB GROUP	Metallized Fuels Solid Fuel Ramjets

19 ABSTRACT (Continue on reverse if necessary and identify by block number)

A series of experiments were conducted to investigate the effects of metallized fuel composition on the combustion characteristics of solid fuel ramjets (SFRJ). Metallized fuels were burned in a two dimensional SFRJ motor under conditions similar to the actual flight conditions proposed for solid fuel ramjets. Pressure, air inlet temperature and flowrate measurements were taken using an automatic data acquisition system. High speed motion pictures were taken of the interior of the combustor during the burning of the solid fuel through two viewing windows located in the recirculation zone and just prior to the aft mixing chamber where the boundary layer was more fully developed. Tests were conducted at mass fluxes of 0.2 and 0.5 lbm/in^2 sec, with pressures ranging from 57 to 200 psia and with a nominal inlet air temperature of 1100°R.

20 DISTRIBUTION/AVAILABILITY OF ABSTRACT	21 ABSTRACT SECURITY CLASSIFICATION
☐ UNCLASSIFIED/UNLIMITED ☐ SAME AS RPT ☐ DTIC USERS	Unclassified

22a NAME OF RESPONSIBLE INDIVIDUAL	22b TELEPHONE (Include Area Code)	22c OFFICE SYMBOL
David W. Netzer	(408) 646 2980	67Nt

DD FORM 1473, 84 MAR 83 APR edition may be used until exhausted
All other editions are obsolete

SECURITY CLASSIFICATION OF THIS PAGE

19. ABSTRACT (continued)

The surface of fuels had a characteristic shedding of small, unignited flakes. The flakes are thought to be binder material, and were more prevalent at lower pressures. Occasional shedding of large surface layers was observed, especially during motor shutdown. Metallic surface agglomerations appeared to interact strongly with these irregular surface layers. Large magnesium particles exhibited the expected bright ignition characteristics. Boron particles were not observed, apparently because they were smaller than the resolution limits of the motion pictures.

Approved for public release; distribution is unlimited.

The Effects of Metallized Fuel Composition on the Combustion Characteristics of Solid Fuel Ramjets

by

Adonis Karadimitris
Lieutenant, Hellenic Navy
B.S., Hellenic Naval Academy, 1977

Submitted in partial fulfillment of the
requirements for the degree of

MASTER OF SCIENCE IN ENGINEERING SCIENCE

from the

NAVAL POSTGRADUATE SCHOOL
December 1986

ABSTRACT

A series of experiments were conducted to investigate the effects of metallized fuel composition on the combustion characteristics of solid fuel ramjets (SFRJ). Metallized fuels were burned in a two dimensional SFRJ motor under conditions similar to the actual flight conditions proposed for solid fuel ramjets. Pressure, air inlet temperature and flowrate measurements were taken using an automatic data acquisition system. High speed motion pictures were taken of the interior of the combustor during the burning of the solid fuel through two viewing windows located in the recirculation zone and just prior to the aft mixing chamber where the boundary layer was more fully developed. Tests were conducted at mass fluxes of 0.2 and 0.5 lbm/in^2 sec, with pressures ranging from 57 to 200 psia and with a nominal inlet air temperature of 1100°R.

The surface of most fuels had a characteristic shedding of small, unignited flakes. The flakes are thought to be binder material, and were more prevelent at lower pressures. Occasional shedding of large surface layers was observed, especially during motor shutdown. Metallic surface agglomerations appeared to interact strongly with these irregular surface layers. Large magnesium particles exhibited the expected bright ignition characteristics. Boron particles were not observed, apparently because they were smaller than the resolution limits of the motion pictures.

TABLE OF CONTENTS

LIST OF TABLES

LIST OF FIGURES

ACKNOWLEDGEMENTS

I would like to express my appreciation to Professor David W. Netzer for his invaluable guidance and assistance without which this project couldn't have been completed. Appreciation is also expressed to Professor R. Wood for his interesting comments on the results of this project. Special thanks to Mr. P. J. Hickey and Mr. Don Harvey for their technical assistance.

I. INTRODUCTION

The ramjet, so called because of the ram action that makes possible its operation, is one of the oldest of the family of jet propulsion systems. Because of its characteristics it is considered as one of the most promising jet engines for the future propulsion of missiles or aircraft at supersonic speeds. The ramjet employs no moving parts and consequently it is simple, relatively inexpensive to fabricate and it can obtain high flight speeds that cannot be obtained by other airbreathing propulsion systems. It uses inlet air as a sourse of oxygen and therefore its fuel efficiency is high. [Refs. 1,2: pp. 349, 4]

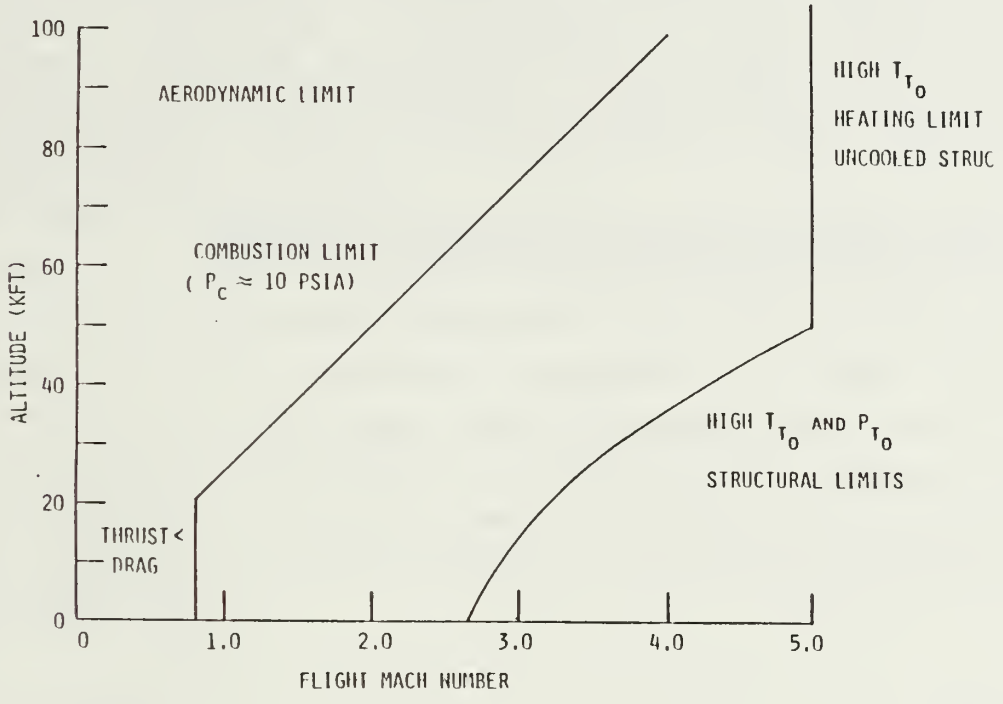

Figure 1.1 Performance Range of Ramjets (Adapted from Ref. 3).

As far as the fuel is concerned there are two main types of ramjet engines, the liquid fuel ramjet (LFRJ) and the solid fuel ramjet (SFRJ). Several characteristics of the solid fuel ramjet indicate that it may be superior to other forms of propulsion for tactical weapons used at intermidiate ranges and supersonic speeds [Ref. 4: p. 7]. But

in order to be an effective propulsion system, the solid fuel ramjet has to demonstrate combustion stability and efficiency inside the expected operating envelope of altitudes and Mach numbers.

Various solid fuels have been studied and used during the past decade of development of the solid fuel ramjet. Non-metallized fuels have received considerable attention and their behavior has been reasonably well characterized. Metallized fuels (Boron, etc) can offer significant gains in performance for applications in which exhaust smoke is not a factor. Little is known about the combustion characteristics of these fuels and, therefore, no models are available for conducting trade-off and design studies. Fundamental data are needed about the effects of fuel composition and flow environment on the surface and gas phase combustion process in order to provide the input to practical combustion / regression rate models.

This investigation was directed at obtaining some of the needed fundamental data on surface regression and particle burning characteristics as influenced by the air mass flux (G), operating pressure and the fuel composition. Data were obtained by an automatic data acquisition system and pictures were taken with two high speed motion picture cameras. Analysis of the results of the experiments revealed a variety of interesting combustion events, related to the surface regression and particle burning, which affect the combustion efficiency and the losses of the SFRJ.

II. BACKGROUND

A. RAMJET ENGINE OPERATING PRINCIPLE

The ramjet engine is the simplest air breathing power plant. It consists mainly of a *diffuser*, through which air is admitted to the engine and in which the velocity is reduced and ram pressure is developed, a *fuel injection system* (liquid fuel ramjets) with which fuel is introduced, vaporized and distributed, and a *combustor* which includes a flameholder, a combustion zone where heat is released and a nozzle through which the burned gases are ejected rearward at high velocity (see Figure 2.1). The liquid fuel ramjet engine generally requires a fuel control system to adjust the fuel flow rate as the air flow rate varies with missile altitude and flight speed. In the solid fuel ramjet the fuel is inside the combustor, around the wall, in the form of a perforated cylinder to permit air to flow through it. No fuel injection or control system is required. In addition, for both the LFRJ and the SFRJ, an *auxiliary power plant*, usually a rocket, must be provided to accelerate the missile or the aircraft to a speed at which the ramjet can provide useful thrust. [Ref. 3]

Figure 2.1 illustrates schematically the operation of a ramjet engine. It is assumed that the engine is immersed in a uniform air stream. [1] A portion of the air stream enters into the combustor (internal flow), reacts with the fuel and expands out the exhaust nozzle. The result of this is a net axial force on the vechicle, collinear with the longitudinal axis of the engine, acting in the forward direction (oposite to the free-stream velocity V_0). This is called the gross thrust (F_g). The net thrust (F_n) is the vector summation of the gross thrust and the external drag (D_e) which is a net axial force arising from the interactions between the external flow and the external surfaces of the ramjet engine:

$$F_n = F_g - D_e. \qquad \text{(eqn 2.1)}$$

[1] This description is for an inlet air stream with the same diameter as the projected frontal area of the inlet. At any other Mach number or angle of attack the inlet air stream will generally be less than the projected frontal area. The axial component of the integral of pressure over the surface area of the external stream tube results in a drag term, called additive drag.

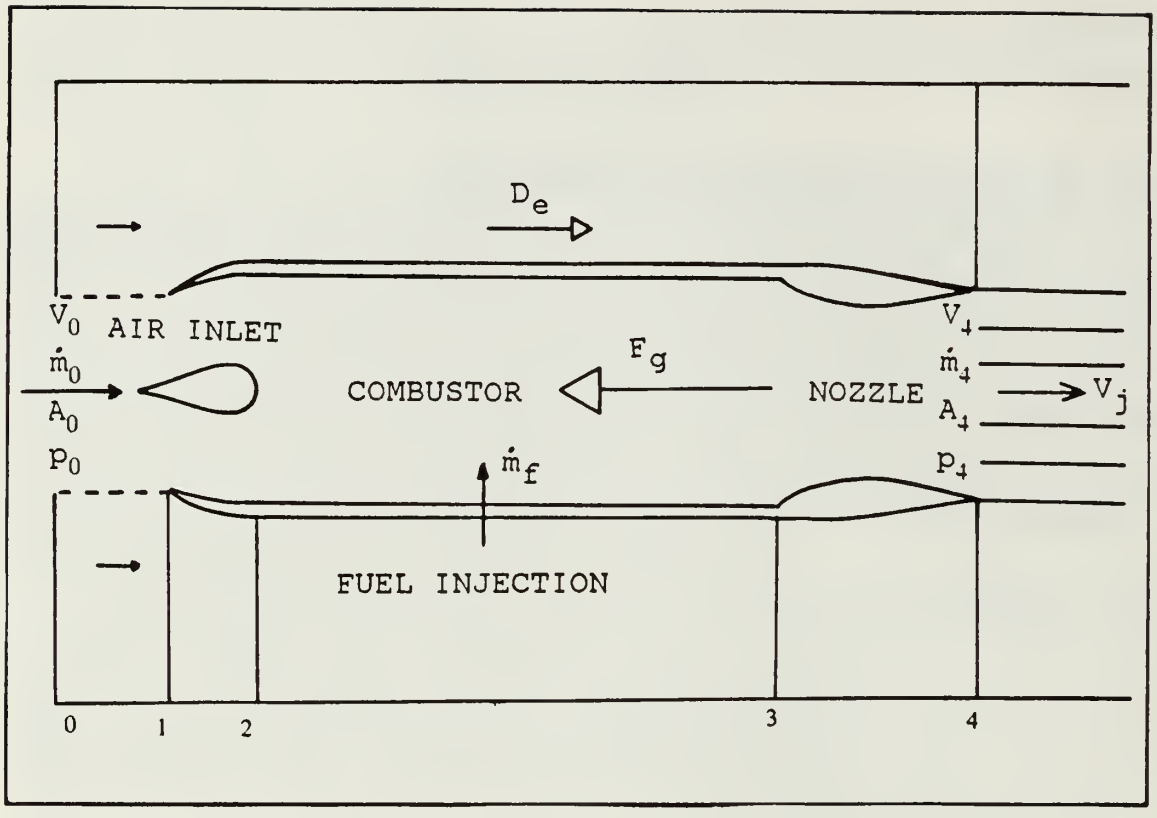

Figure 2.1 Ramjet Airflow Diagram at Design Mach Number.

Since the external drag is related to the missile's aerodynamics, it not discussed here. The gross thrust is equal to the difference between the values of the stream thrust for the internal flow measured at stations 4 and 0 respectively, less the product of the ambient pressure p_0 times the difference between the cross-sectional areas A_4 and A_0 (see Figure 2.1):

$$F_g = \vec{f}_4 - \vec{f}_0 - p_0(A_4 - A_0). \qquad \text{(eqn 2.2)}$$

It can be shown that the above equation can be written:

$$F_g = \dot{m}_4 V_4 - \dot{m}_0 V_0 + A_4(p_4 - p_0). \qquad \text{(eqn 2.3)}$$

By defining the effective jet velocity (V_j) as

$$V_j = V_4 + A_4(p_4 - p_0)/\dot{m}_4, \qquad \text{(eqn 2.4)}$$

and noting that $\dot{m}_4 = \dot{m}_0 + \dot{m}_f$ and $f = \dot{m}_f / \dot{m}_0$ (where $\dot{m}_f$ is the fuel mass flow rate and f is the fuel-to-air ratio), the previous equation for the gross thrust can be written as:

$$F_g = \dot{m}_0 V_0((1+f)V_j/V_0 - 1). \qquad \text{(eqn 2.5)}$$

For a fixed geometry ramjet engine the gross thrust, and consequently the net thrust, is a function of the flight altitude, flight Mach number, fuel-to-air ratio and effective jet velocity. The later depends on the area ratio and efficiency of the exhaust nozzle, the total pressure (P_3) and the total temperature (T_3). The total temperature depends on the fuel-to-air ratio and the type of fuel burned. Since the combustor has no moving parts it can be subjected to high temperatures and stoichiometric fuel-to-air ratios may be utilized. [Ref. 1: pp. 352-368]

B. ENGINE AND COMBUSTION CHARACTERISTICS OF THE SFRJ

The solid fuel ramjet (see Figure 2.2 [Ref. 5]) in general consists of a hollow cylinder in which a cylindrical fuel grain, often with circular port cross-section, is placed [Ref. 6: p. 5].

> The principles underlying the combustion of the SFRJ are: (1) developing a stable, high temperature recirculation zone to ensure flameholding; (2) providing a combustor length-to-diameter ratio adequate to permit full flame spreading within the combustor; and (3) achiving satisfactory mixing of vaporized fuel and air to ensure complete reaction before the combustion gases exit through the exhaust nozzle. [Ref. 7: p. 12]

Usually the following geometry is employed (see Figure 2.2):

1. Head End

The head end consists of the air inlet and the rearward facing step. As the inlet air enters the combustor, a sudden expansion occurs at the rearward facing step which provides the flame stabilization (see Figure 2.3 [Ref 8]). The flame stabilization (flameholding) is very important in the solid fuel ramjet for two reasons. First, the port velocity is very large because the solid fuel ramjet (usually) operates at relatively low chamber pressure, and second, the oxygen for the combustion is provided by the incoming air, which corresponds to a severly diluted oxygen. [Ref. 9]

There are three parameters that affect the combustion limits for a given fuel composition (see figure 2.4). The first is the ratio of the fuel port area (A_p) to the area of the air injector (A_i). Combustion can be sustained if the injector area (A_i) is

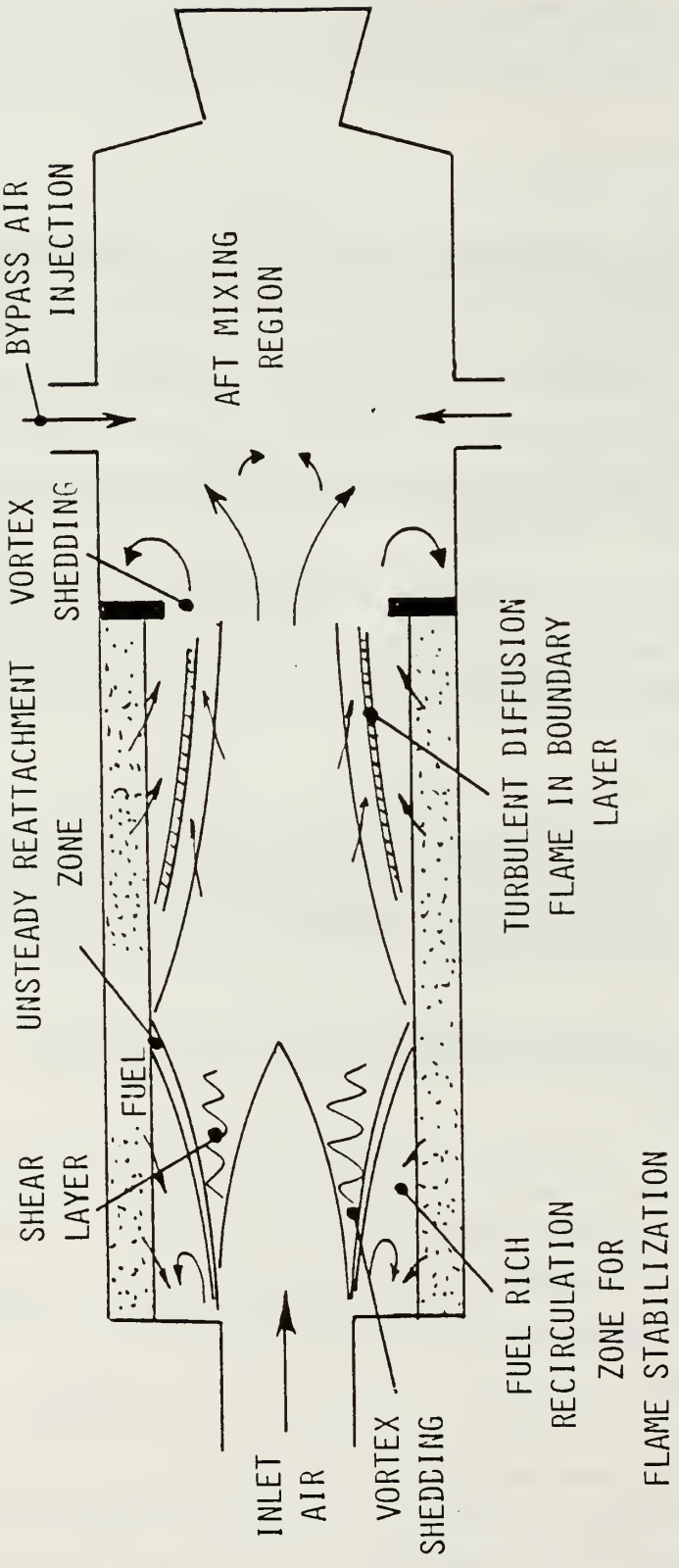

Figure 2.2 Solid Fuel Ramjet Engine (Ref. 5: p. 43).

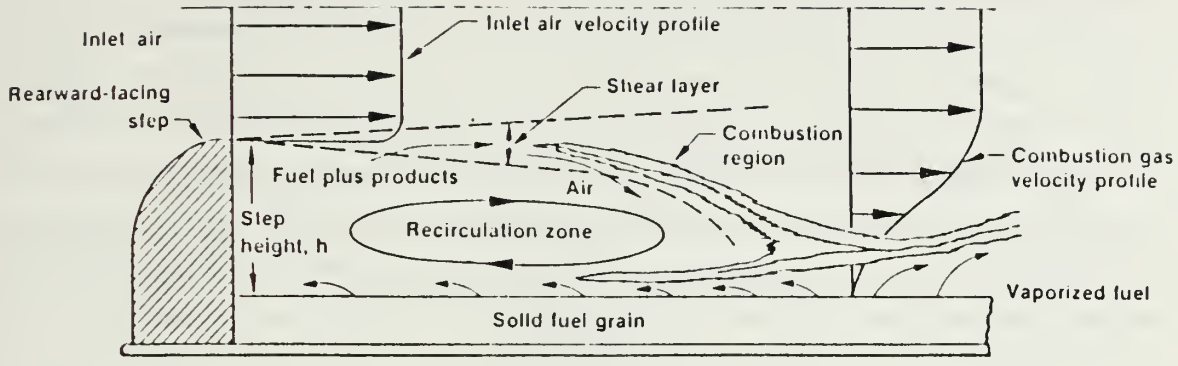

Figure 2.3 Flow Field in the Flame Stabilization Region (Ref. 8).

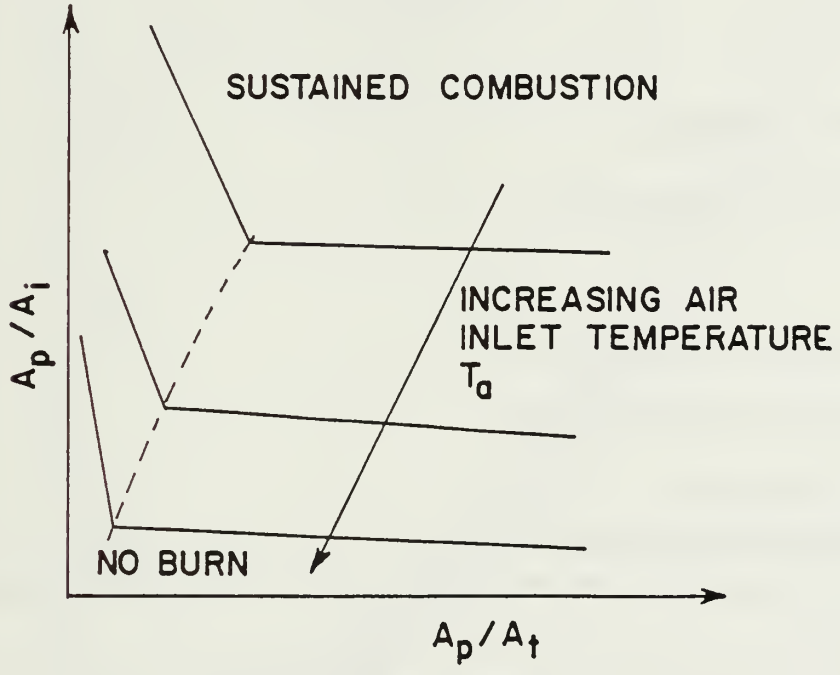

Figure 2.4 Typical Flamability Limits for the SFRJ (Ref. 5: p. 52).

sufficiently small with respect to the port area (A_p), which means that a large step height (h) is needed. However, the larger is the step height, the larger the losses in inlet stagnation pressure [Ref. 10: p. 1]. Inlet stagnation pressure losses reduce the overall performance of the solid fuel ramjet. Recearch by the United Technologies in the field of flame stabilization led to the development of inlets, such as the tube-in-hole injector, which minimize the required inlet step height and decrease the effects of inlet distortion [Ref. 4: p. 7]. The second parameter is the velocity in the fuel grain port, which is

controlled by the ratio of the fuel port area (A_p) to the nozzle throat area (A_t). If the port velocity exceeds some limiting value, blowoff occurs. The third parameter is the inlet air stagnation temperature (see Figure 2.5) which in turn is a function of flight Mach number and altitude. At higher flight Mach numbers, the stagnation temperature of the air is higher, so flame stabilization is achieved more easily. The maximum value of the flight Mach number is limited by the structural limits of the missile (see figure 1.1). Figure &temp shows the effect of flight Mach number and altitude on the stagnation temperature, based on the assumption that $\gamma = 1.4$ and on the formula:

$$T_t = T_0(1+((\gamma-1)/2)M_0^2) \qquad \text{(eqn 2.6)}$$

where:

T_t = stagnation temperature

T_0 = temperature at a given altitude

$\gamma = C_p/C_v$

C_p = specific heat at constant pressure

C_v = specific heat at constant volume

M_0 = flight Mach number

2. **Main Combustor Section**

The main combustor section is a hollow cylinder which contains the solid fuel grain.

The sudden expansion, discused already, generates two distinct flowfields within the fuel grain. In the first one, the recirculation zone, whose size is determined by the hight of the rearward facing step, the flow is highly turbulent and fuel rich. This hot gas region provides the energy necessary for sustaining the combustion process which must occur further downstream [Ref. 10: p. 1]. In the second flowfield (downstream of the flow reattachment) a boundary layer flow is formed along the fuel grain. The free stream along the center-line of the engine is oxygen (air) rich, and the gas near the wall is fuel rich. The result of this is a diffusion flame within the boundary layer relatively close to the fuel surface. Due to that diffusion flame, heat is transferred

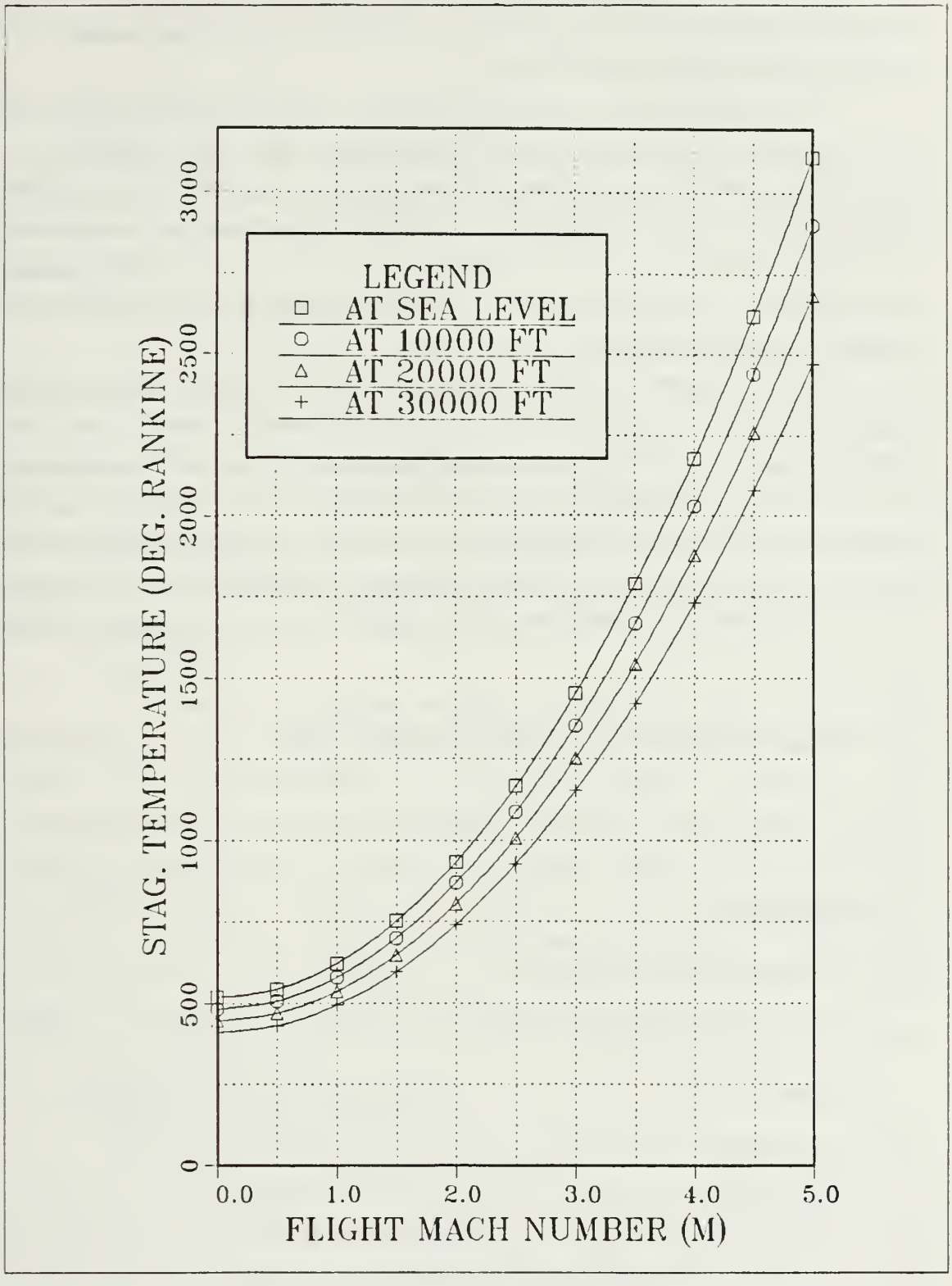

Figure 2.5 Stagnation Temperature vs. Flight Mach Number.

by convection and radiation to the solid fuel which causes vaporization or decomposition of the fuel. The gaseous fuel products of this process react with the air and burn in the gas phase. [Ref. 6: p. 5]

The regression rate of the solid fuel (rate at which the solid fuel recedes during the combustion), is determined mainly by the air mass flux in the combustor and by the inlet air temperature. Since these parameters vary as a function of the altitude and Mach number of the missile, the regression rate in the SFRJ combustor varies in flight. As the flight altitude increases the air mass flow rate decreases and consequently, the fuel flow rate is automatically reduced. This phenomenon makes the SFRJ exibit a degree of self-throttling. [Ref. 7: p. 16]

The fuel regression rate is proportional to the total heat transfer from the diffusion flame to the surface of the solid fuel. The convective heat transfer depends primarily on the air mass flow and on the air temperature. The radiative heat transfer is a function of the combustor pressure, combustion zone thickness, and flame temperature. Analysis of several hundred tests, most of which employed an all hydrocarbon fuel made by the United Technologies / CSD [Ref. 7: p. 16], showed that the regression rate of the solid fuel can be derived from the following semiempirical equation:

$$\dot{r} \sim (\dot{Q}_{conv} + \dot{Q}_{rad}) \sim (G^{0.6}\, T_a^{0.3}\, D^{-0.4} + (1-e^{\alpha P \delta})T_f^4) \qquad \text{(eqn 2.8)}$$

where:

$\dot{r}$ = regression rate

$\dot{Q}_{conv}$ = convective heat transfer

$\dot{Q}_{rad}$ = radiative heat transfer

G = fuel port mass flux

T_a = air temperature

D = port diameter

α = constant of proportionality

P = combustion pressure

T_f = flame temperature

δ = diffusion zone thickness.

Usually the self-throttling is not enough to maintain optimum fuel-to-air ratio as the altitude and or the Mach number is varied. Some control of the fuel regression rate may be possible through the use of swirl generators and or variable bypass air designs. [Ref. 6: p. 7]

3. **Aft Mixing Chamber**

A portion of the fuel that leaves the surface of the grain never reaches the diffusion flame. It remaines below the flame near the wall. The boundary layer exits from the aft end of the fuel grain and may result in decreased combustion efficiency if the fuel is not consumed before entering the exhaust nozzle. The combustion efficiency can be increased if an aft mixing chamber downstream of the fuel grain is used. This allows additional chemical reaction of the unburned fuel to take place. To promote mixing in that region and to increase the allowable fuel loading, a portion of the inlet air is sometimes bypassed to the region aft of the fuel grain [Ref. 10: p. 2].

4. **Exit Nozzle**

The nozzle converts the enthalpy of combustion into kinetic energy [Ref. 11: p. 111] to provide the required thrust for sustaining the missile's forward motion. It is often considered to be part of the combustor, because it is often convenient to manufacture the two components as part of the same assembly. Usually, a fixed throat area nozzle is employed for the ramjet engine. However, the use of a two-position nozzle could optimize the ramjet performance for two different thrust levels. It is also possible to design continuously variable nozzles that could optimize the performance at all flight conditions. In practice, however, the complexity and the weight of such nozzles rarely justify these approaches. [Ref. 2: p. 38]

C. METALLIZED FUELS

1. High Energetic Performance Fuels

Most often the SFRJs employ hydrocarbon (HC) fuels, usually polymers, e.g., polybutadiene (PB), polyethylene (PE), polymethylmetacrylate (PMM-"Plexiglas"), etc. They have been used extensively and, therefore, are well understood. However, the use of highly metallized fuels can provide higher energetic performance. [Ref. 6: pp. 5, 10]

The evaluation of the energetic performance of an air breathing engine is based on the criteria of the specific impulse (I_{sp}) and thrust specific fuel consumption (TSFC). For convenience, however, usually the static specific impulse ($I_{sp,s}$) is used as a measure of combustor performance. For a ramjet engine the static specific impulse is proportional to the heat release per unit mass of fuel (q_R), also called heat of combustion, which is calculated in terms of the standard enthalpy change during a complete reaction with gaseous oxygen:

$$q_R = -\Delta H^\circ_R. \qquad \text{(eqn 2.9)}$$

The negative sign is used because the enthalpy of reaction is negative for an exothermic reaction. Thus, the energetic performance of a ramjet propulsion system can be characterized by the energy released per unit mass of the fuel ($-\Delta H^\circ_R$). However, in many SFRJ systems, limitations on the space availability for the solid fuel indicate that the energy release per unit volume, also called energy density ($-\rho\Delta H^\circ_R$), should be used as the main criterion in selecting the appropriate fuel combination. [Ref. 6: pp. 1-4]

Figure 2.6 [Ref. 6: p. 12], presents the heat of combustion of elements with oxygen per unit mass and per unit volume. For comparison, represetative values for a hydrocarbon fuel of a general formula CH_2 (i.e., polyethylene or polybutadiene) which represents a high energy hydrocarbon with $-\Delta H^\circ_R = 10.5$ kcal/g, are also shown. Berillium (Be) and boron (B) exibit higher energy of combustion per unit mass and per unit volume than hydrocarbons. However, there are a number of other solid elements with high energy densities, but relatively low heat of combustion per unit mass. [Ref. 6: pp.11-15]

> Metal hydrides may be very attractive as the the existence of hydrogen in their molecule usually increases the heat of combustion per unit mass over that of the metal itself. Among the metal hydrides berillium hydride has the highest heat of combustion per unit mass (18.13 kcal/g), higher than any metal. The solid borane ($B_{10}H_{14}$) also exhibits very high heat of combustion per unit mass (over 15.5 kcal/g). However, most metal hydrides have very low density (usually less than 1 g/cc) except for zirconium hydride (ZrH_2) with $\rho = 5.67$ g/cc and titanium hydride (TiH_2) with $\rho = 3.9$ g/cc. [Ref. 6: p. 16]

Metal alloys and other metal compounds may have an advantage over the corresponding mixing of the individual elements when considering density, availability,

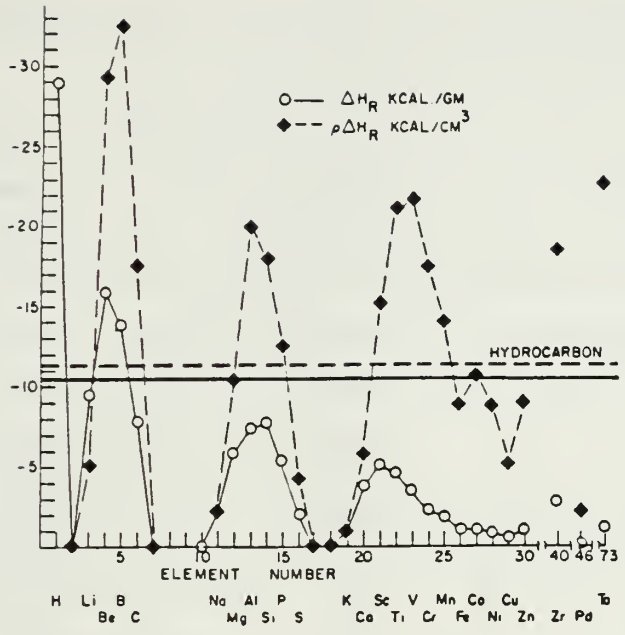

Figure 2.6 Heat of Combustion of Elements (Ref. 6: p. 12).

and ignition and combustion characteristics. In adition they may have very high energetic potential. Boranes, metal-metal compounds, carbides, and metal phosphites are the most interesting metals. [Ref. 6: pp. 16-22]

Manufacturing and combustion process considerations should be taken into account for the final selection of fuel ingredients for the SFRJ. Table 1 [Ref. 6: p. 29] shows the most energetic fuel candidates for the SFRJ.

2. **Combustion Characteristics of Metallized Fuels**

Regardless of the promising potential, the practical use of the highly metallized fuels for the SFRJ presents severe problems associated with complex burning phenomena, affecting the energy generation process which may result in poor SFRJ performance.

Combustion studies of metallized fuels for SFRJs have shown that even though the flow characteristics are similar for both the non-metallized and the metallized fuels, there are some differences that characterize the combustion process of solid fuel formulations highly loaded with metal particles. [Refs. 12,13: pp. 6-11, 20-40]

Metal particles tend to accumulate and can form relatively large agglomerates on the surface of the solid metallized fuel prior to their ejection into the gas stream.

TABLE 1

THE MOST ENERGETIC FUEL CANDIDATES FOR THE SFRJ (REF. 8)

FUEL	$-\Delta H^{\circ}_{R}$ (kcal/g)	$-\rho\Delta H^{\circ}_{R}$ (kcal/g)
AlB_{12} (alloy)	12.16	32.93
B	13.87	32.6
AlB_{12}	12.45	32.93
B_4C	12.7	31.07
MgB_{12}	12.4	30.2
TiB_2	6.45	29.02
VB_2	5.7	29
B_6Si	11.6	28.6
TaB_2	2.49	27.71
ZrB_2	4.28	26.07

Even though the particles or fragments that leave the fuel surface are very hot, they usually do not ignite until they are away from the surface into the oxygen rich region of the combustor. The ignition takes place abruptly and creates a bright flame bursting from the particle, which releases most of the energy. The boundary layer gas phase diffusion flame is closer to the surface and not as intense as that of non-metallized fuels, and probably plays a less important roll in the overall combustion process. [Ref. 12: pp. 2-16]

III. DESCRIPTION OF APPARATUS

In general, a two-dimentional solid fuel ramjet motor with a vitiated air heater, an igniter and a purge gas system, controlled by a remote station, have been used (see Figure 3.1). A digital data acquisition system with a computer and appropriate software and a printer were used for the adjustments, automatic control, data acquisition, and data reduction. Two HYCAM 16 mm high speed motion picture cameras were used for taking pictures inside the motor during the burn time.

A. TWO-DIMENTIONAL SFRJ MOTOR

The two dimensional motor had four basic sections (see Figures 3.2 and 3.3):

1. The head-end with air inlet and rearward facing step
2. The main combustion section
3. The aft mixing chamber
4. The exit nozzle.

The head-end had a flow straightener followed by inlet step blocks which reduced the flow height. Two pairs of blocks were available providing inlet step heights of 0.25 or 0.325 inches.

The motor chamber was 2.5 inches wide. The solid fuel slabs were placed on the bottom and on the top walls, so it was possible to take pictures of the space between them. The length of the fuel slabs was 16 inches. The port height (distance between opposing fuel slabs) was about 1 inch, depending on the thickness of the fuel slabs. One of the side walls of the motor had three viewing windows (see Figure 3.4) positioned at the reattachment point, the mid-chamber and just prior to the mixing chamber (in the boundary layer combustion region). The first and the third of these windows were used for taking pictures of the interior of the motor, simultaneously, during burning of the solid fuel. These viewing ports consisted of 0.25 inch Plexiglas windows, an air injection system to purge the windows and metal shields to partially cover the window ports to prevent the windows from fowling or burning during the combustion process. The air purge system consisted of a high pressure bottle with compressed air ($P > 500$ psia) which was controlled remotely through a valve. The air flowed through a sintered ring which was located beteen the Plexiglas and the metal shield of the viewing window. The metal shield was a 1.5 inch diameter steel plug with

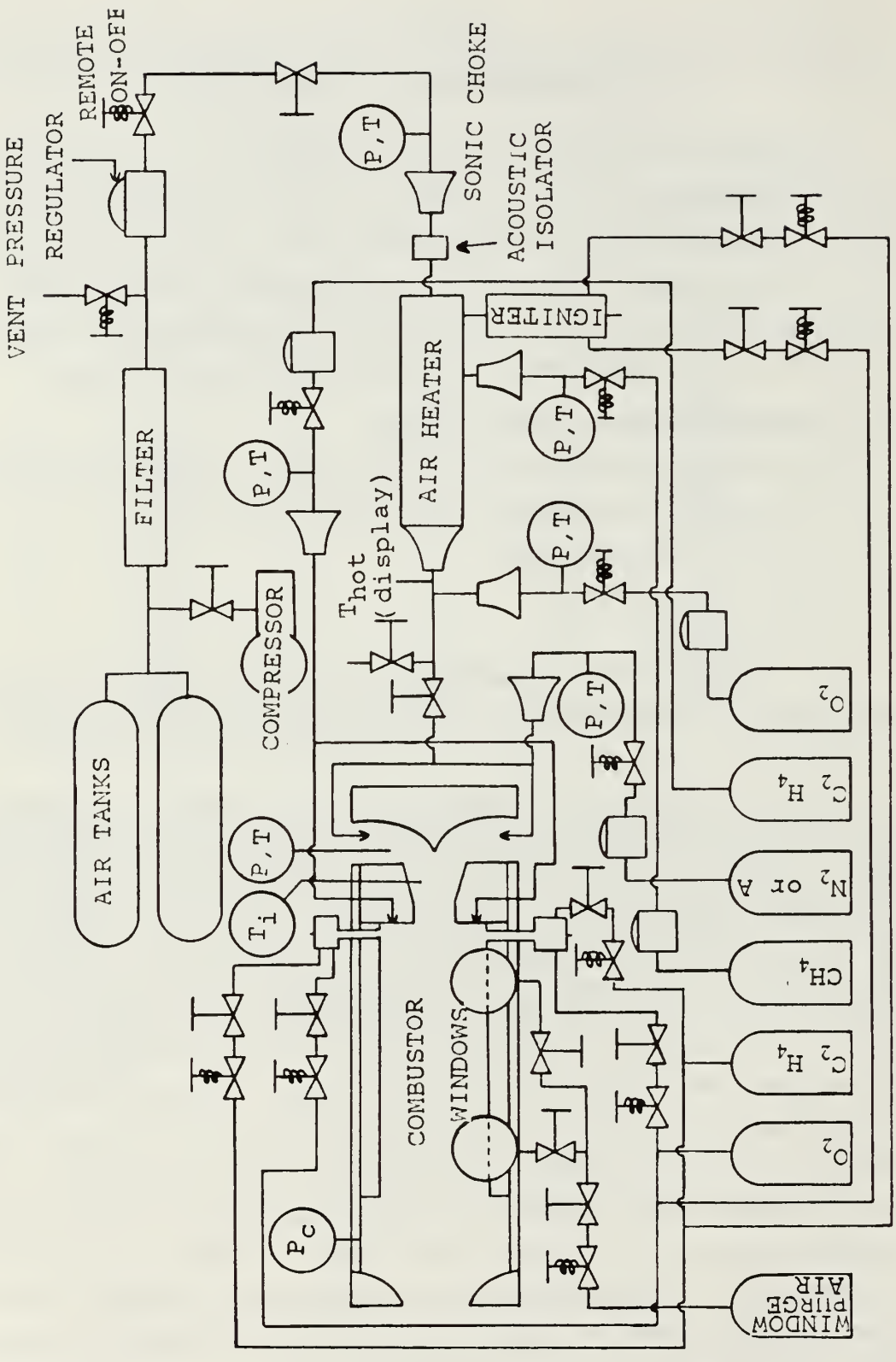

Figure 3.1 SFRJ Functional Block Diagram.

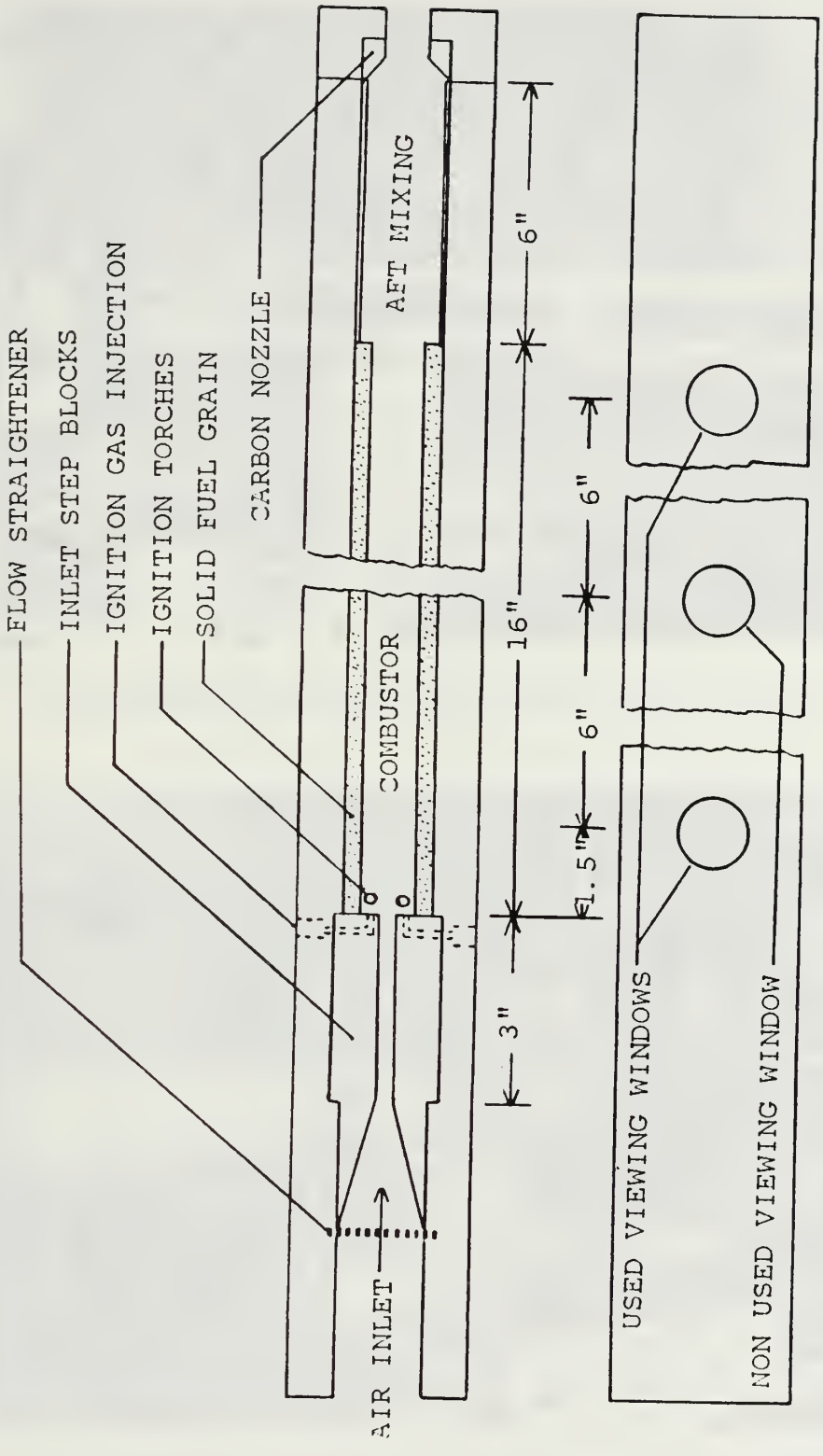

Figure 3.2 Schematic of the SFRJ Motor (Ref. 13: p.14).

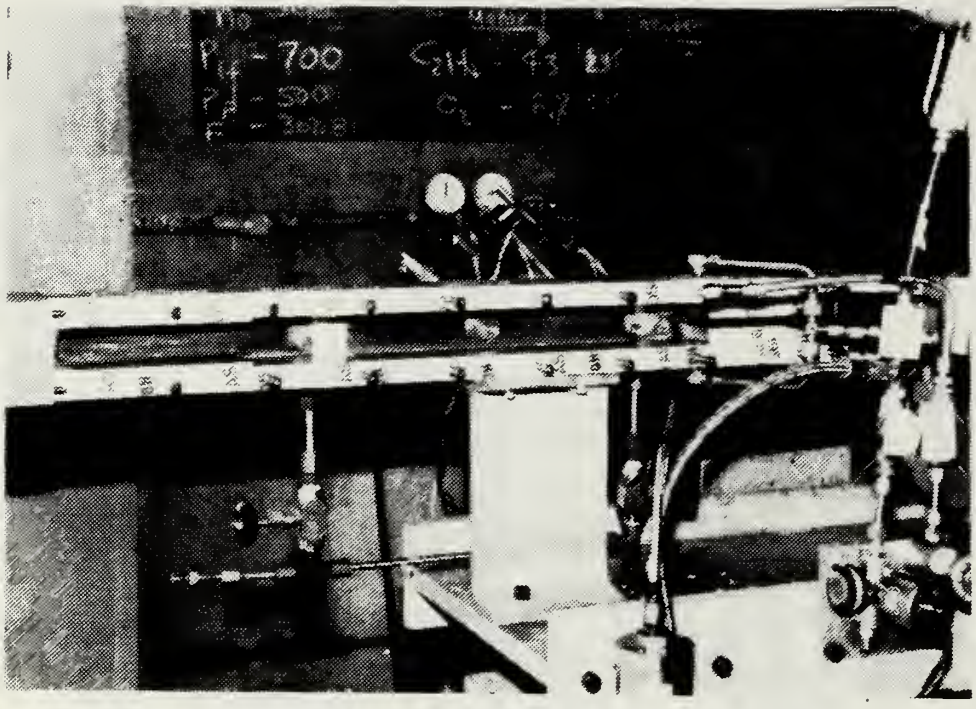

Figure 3.3 SFRJ Motor Side View with Right Side Removed.

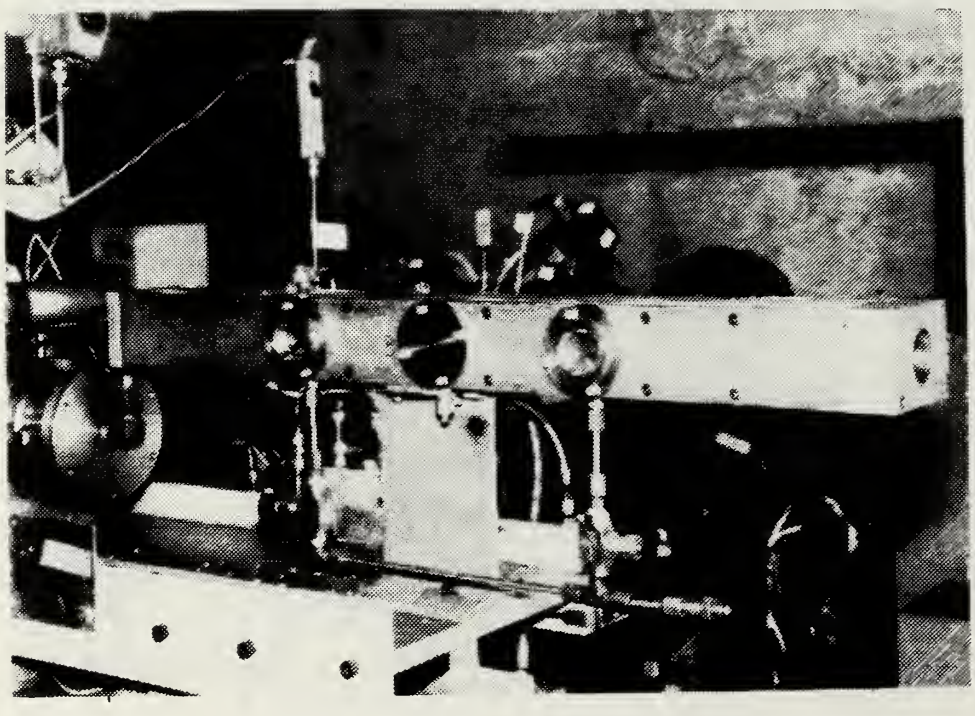

Figure 3.4 Viewing Windows on the Left Side of the SFRJ.

a 0.5 inch hole drilled in it to allow viewing of the metallized fuel surface. In a previous investigation nitrogen had been used instead of air, but it was found to quench the combustion process. The mass flow rate of purge gas for the viewing windows was adjusted through local manual controls before firing. The fine adjustment of the mass flow rate of the purge gas for the front viewing window proved to be of great importance because with a low mass flow rate it was impossible to keep the window clean and with a high mass flow rate it was impossible to ignite the motor.

The aft mixing chamber (downstream of the fuel) was a chamber with dimensions 6 in × 2.5 in × 1.25 in. Here the reaction between the fuel and the air was enhanced due to better mixing and increased residence time.

The nozzle block was at the end of the motor. Various diameter carbon nozzles could be inserted into the nozzle block. The exit nozzle diameter was used to adjust the pressure inside the combustion chamber for any specified air mass flowrate, and also to keep the combustion process within the flammability limits.

TABLE 2
CARBON NOZZLE DIAMETERS (INCHES)

0.75
0.85
0.95
1.125
1.35
1.50

Table 2 shows the diameters of the carbon nozzles that were utilized.

B. VITIATED AIR HEATER

A schematic of the vitiated air heater system used to simulate actual flight conditions for the solid fuel ramjet is shown in Figure 3.5. It was designed to supply air at any desired mass flow rate within the system limitations (about 4 lbm/sec) and at any temperature up to approximately 1500°R. The heater output was connected to the input of the solid fuel ramjet. High pressure (3000 psi) air tanks were the primary air supply and the mass flow rate was regulated by means of a sonically choked

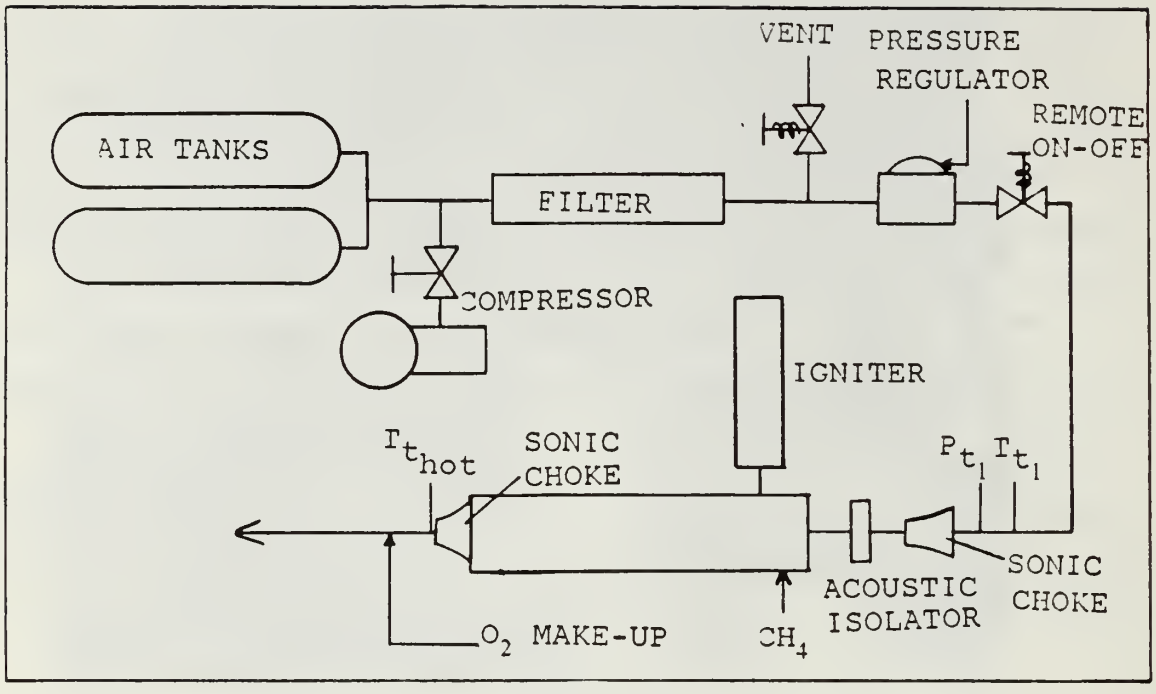

Figure 3.5 Schematic of the Vitiated Air Heater.

converging nozzle. As the air was passing through the choked flow nozzle, P_{t_1} and T_{t_1} were meassured. Using these measurements the computation of the mass flowrate was accomplished using conservation of mass for choked sonic flow:

$$\dot{m}_{air} = (C_D P_{t_1} A^* F_1) / \sqrt{(R T_{t_1} / g_c)} \qquad \text{(lbm/sec)} \qquad \text{(eqn 3.1)}$$

where:

$$F_1 = \sqrt{(\gamma (2/(\gamma+1))^{((\gamma+1)/(\gamma-1))})} \qquad \text{(eqn 3.2)}$$

$$A^* = (\pi d^{*2})/4 \quad (in^2) \qquad \text{(eqn 3.3)}$$

d^* = sonic choke diameter

C_D = discharge coefficient ($\sim$ 0.97)

R = individual gas constant

T_{t_1} = measured temperature (°R)

P_{t_1} = measured pressure (psia)

g_c = 32.2 (lbm-ft)/(lbf-sec^2)

Or in another form:

$$m_{air} = C_D P_{t_1} (\pi/4) d^{*2} KM / \sqrt{T_{t_1}} \qquad \text{(eqn 3.4)}$$

where:

$$KM = F_1 / \sqrt{(R/g_c)}. \qquad \text{(eqn 3.5)}$$

The vitiated air heater was fueled by bottled gaseous methane (CH_4). Bottled oxygen (O_2) was used to replace that consumed in the combustion process. The adjustments of the mass flowrate of the heater fuel and oxygen were made through sonic chokes and set pressures according to the choked sonic flow formula described above.

Table 3 gives the values of KM for the different gases that were used in this project for heating, ignition, and purging.

C. IGNITER

Two ethylene-oxygen torches were used for the ignition of the SFRJ combustor. The torches were directed into the recirculation zones in the across-motor direction. Ethylene was also injected into the recirculation zone at the inlet steps to aid the ignition process.

The mass flowrate of the ignition gas (ethylene) was also controlled through a sonic choke and a set pressure according to the choked sonic flow formula.

Once the motor was ignited, the torches and ethylene were shut off and the SFRJ fuel was allowed to burn unaided.

TABLE 3
VALUES OF KM FOR AIR AND GASES

GAS	KM
Air	0.5320
N_2	0.5229
O_2	0.5589
CH_4	0.3876
C_2H_4	0.4985

D. PURGE SYSTEM

Nitrogen (N_2) was used as the purge gas. As the motor run was terminated by dumping the air upstream of the combustor, nitrogen gas was passed through the fuel grain for about 3-6 seconds to ensure extinguishment of the combustion.

E. DATA ACQUISITION SYSTEM

A 3054A computer based Hewlett-Packard acquisition and control system was used (see Figure 3.6). The main parts of this system are a HP-9836 computer system (see Figure 3.7), a 3497A data acquisition and control unit, and two A/D integrating voltmeters (HP-3456A and HP-3437A). [Ref. 14]

1. Calibration of the Transducers

The following pressures were measured with strain gage transducers:

a. P_a : Air sonic choke pressure
b. P_c : SFRJ chamber pressure
c. P_{hf} : Air heater fuel sonic choke pressure
d. P_{ho} : Air heater oxygen sonic choke pressure
e. P_{if} : SFRJ ignition fuel sonic choke pressure.

2. Mass Flow Rate Set-Ups

The set-up of the following mass flow rates was easily made with the computer before the firing by means of set pressures:

a. $\dot{m}_{air}$ (Air mass flowrate)
b. $\dot{m}_{hf}$ (Air heater fuel mass flowrate)
c. $\dot{m}_{ho}$ (Air heater oxygen mass flowrate)

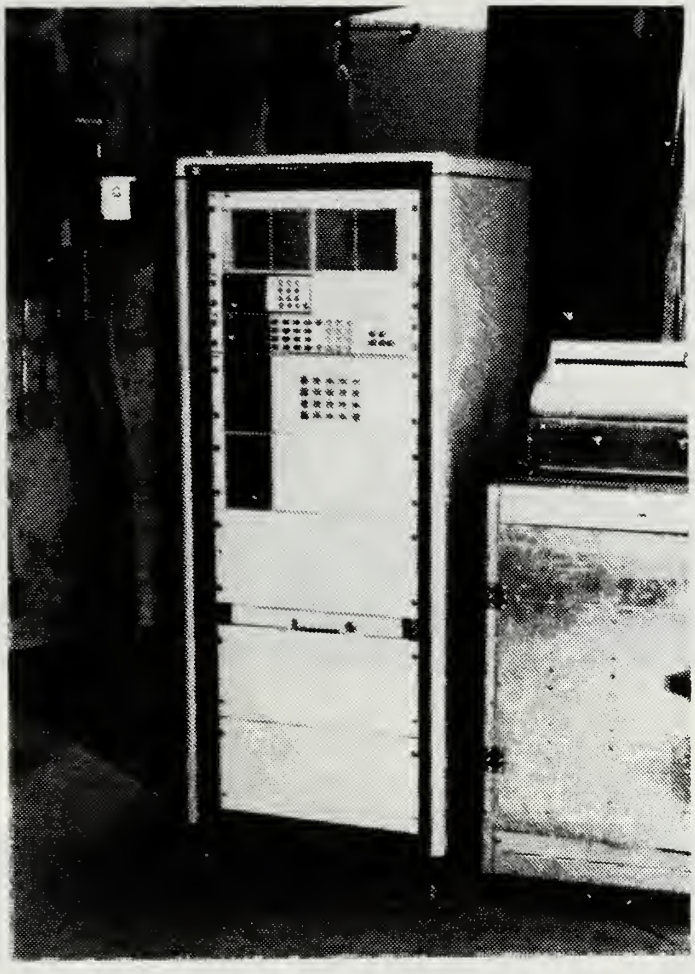

Figure 3.6 Data Acquisition System.

d. $\dot{m}_{if}$ (SFRJ ignition fuel mass flowrate).

3. **Data Extraction**

After each run the following data were displayed by the computer as a function of time (every 0.5 seconds):

a. $\dot{m}_{air}$ (Air mass flowrate)
b. $\dot{m}_{hf}$ (Air heater fuel mass flowrate)
c. $\dot{m}_{ho}$ (Air heater oxygen mass flowrate)
d. $\dot{m}_{if}$ (SFRJ ignition fuel mass flow rate)
e. T_i (Temperature at SFRJ motor air inlet)
f. P_c (SFRJ chamber pressure)
g. P_h (SFRJ head-end pressure)

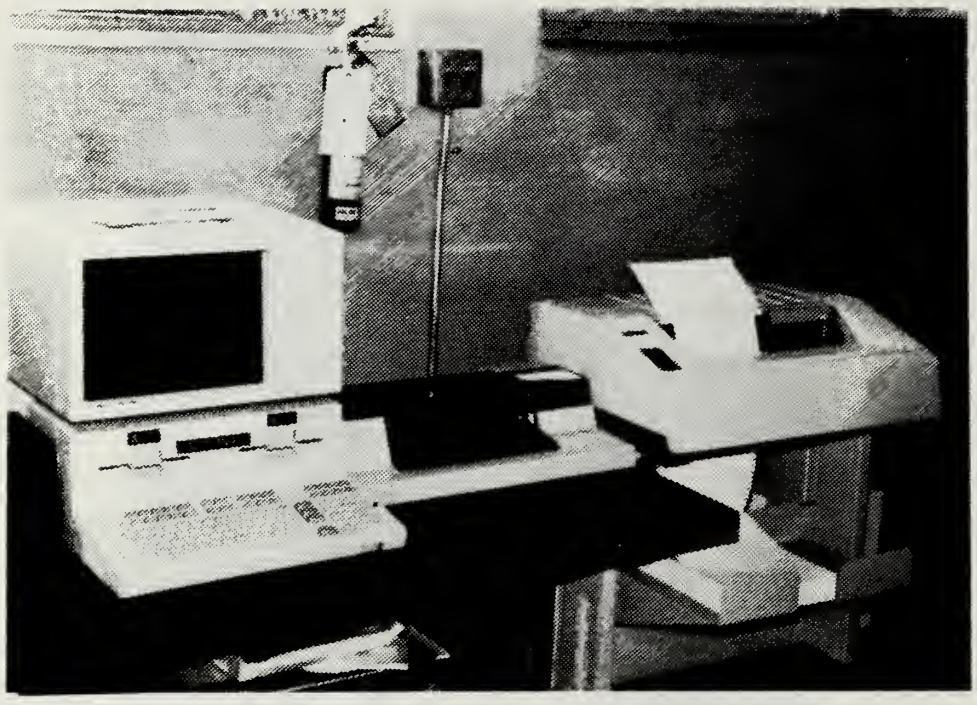

Figure 3.7 Computer and Printer.

h. T_a (Temperature at the air sonic choke).

Appendix A shows a typical printout where the above data and also other information related to each experiment are contained.

F. REMOTE CONTROL PANEL

Figure 3.8 shows the control panel used for the remote operation of the SFRJ. Initiation of the vitiated air heater and the air flow through the SFRJ were made manually. All other test operations were programmed and accomplished by the computer system.

G. HYCAM 16 MM CAMERAS

The two HYCAM 16 mm cameras used in this work (see Figure 3.9) were high speed motion picture cameras manufactured by Red Lake Laboratories.

The design of these cameras is based on the idea of a high speed rotating prism which is combined with a shutter and a film sprocket on a single shaft driven by the film, simulating a drive belt on the take-up motor. The film transport has a film capacity of 400 feet of standard thickness film on daylight loading spools and also it can accept 100 and 200 foot daylight loading spools. In this project the 100 feet capacity was used. [Ref. 15: pp. 3, 4]

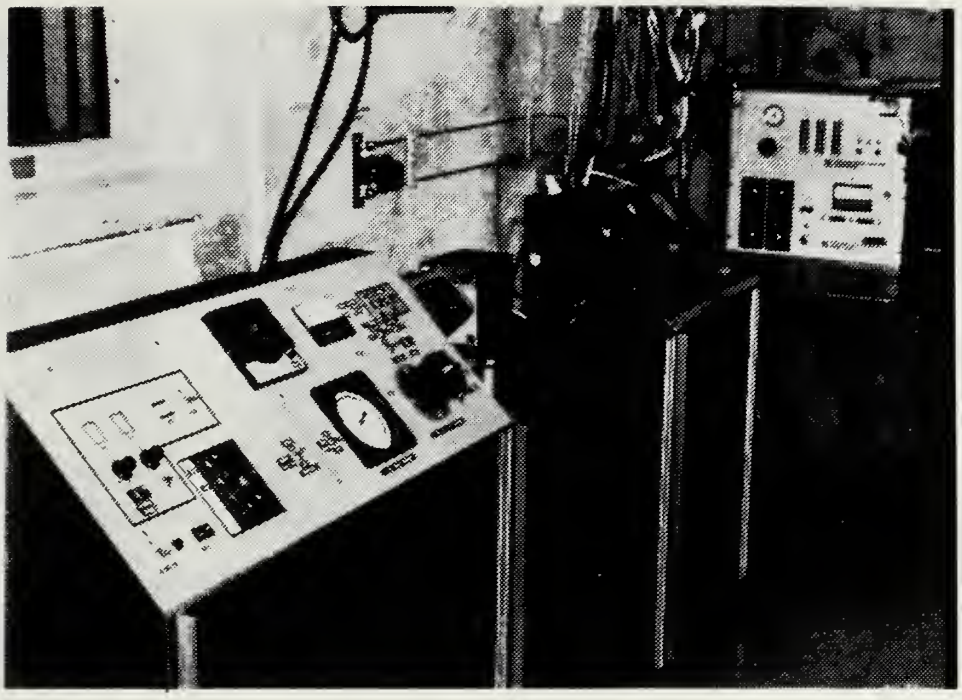

Figure 3.8 Remote Control Panel.

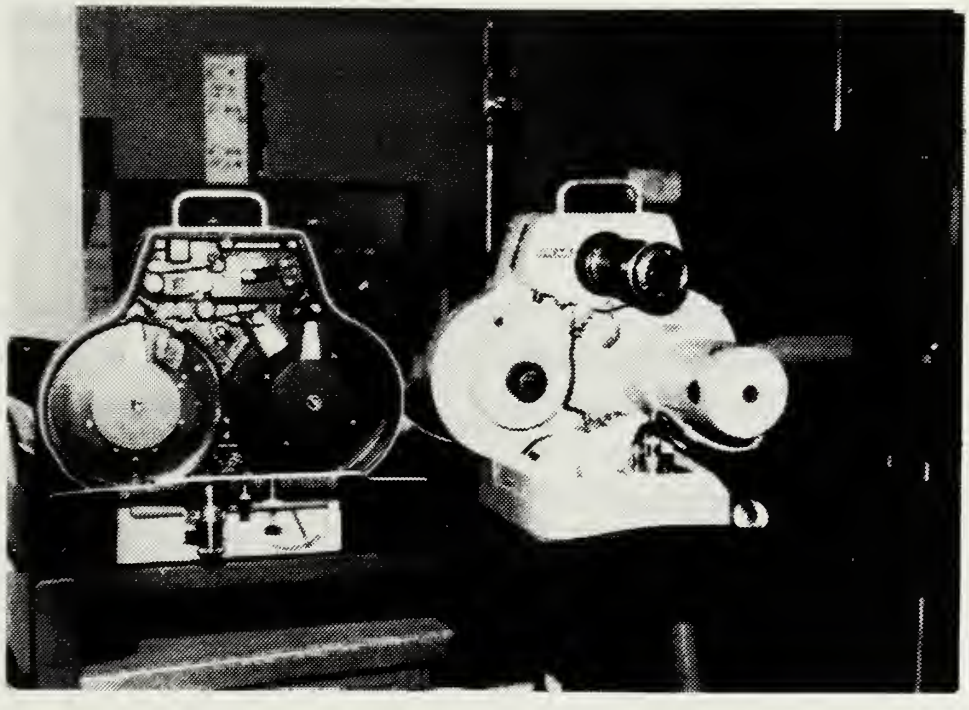

Figure 3.9 Front and Rear View of HYCAM 16 mm Cameras.

The HYCAM speed control is a solid state electronic closed loop servo system which can be manually set to control frame rates. Speeds up to 11000 picures per second (PPS) can be obtained [Ref. 15: pp. 4, 9]. For these experiments a speed of 6000 PPS has been used. The exposure time is given by the formula [Ref. 15: p. 13]:

Exposure Time = Shutter Exposure Ratio × (1/Frame Rate)

For a shutter exposure ratio equal to 1/2.5 and a film speed equal to 6000 PPS the exposure time was:

Exposure Time = (1/2.5) × (1/6000 PPS) ~ 67 μsec.

One of the HYCAM cameras was equipped with a dual emitting diode (LED) timing system, and the other one was equiped with a NE2J neon lamp timing system, for the recording and annotation of film data.

The HYCAM cameras have been designed to withstand moderate vibrations and to operate in any orientation [Ref. 15: p. 7]. In this project the camera that was used for the viewing window of the reattachment zone was installed horizontaly and the other one was installed normaly (see Figure 3.10), in order to match the large size of the two cameras with the small distance (12 inches) between the two viewing windows.

The operations of the two cameras were made simultaneous by a double remote control switch in the control room.

Two zoom-Nikkor 35-105 mm f/3.5-4.5 lenses were used for these cameras. The lenses were mounted on the cameras in reverse through C-mount macro adapter rings to improve the image quality and the working distance between the front of the lens and the subject.

Because of the fact that the information given by the the lens operator's manual was for normal installation, experimental data were extracted prior to the installation of the cameras for the magnification as a function of the distance between the film plane marker on the carrying handle of the cameras and the subject (see Figure 3.11). A magnification of 1:1 was desired in the present investigation. From Figure 3.11 this magnification required a distance of 30 cm between the film plane and the subject.

The depth of field was also experimentally determined for different f/stops as shown in Table 4 and Figure 3.12.

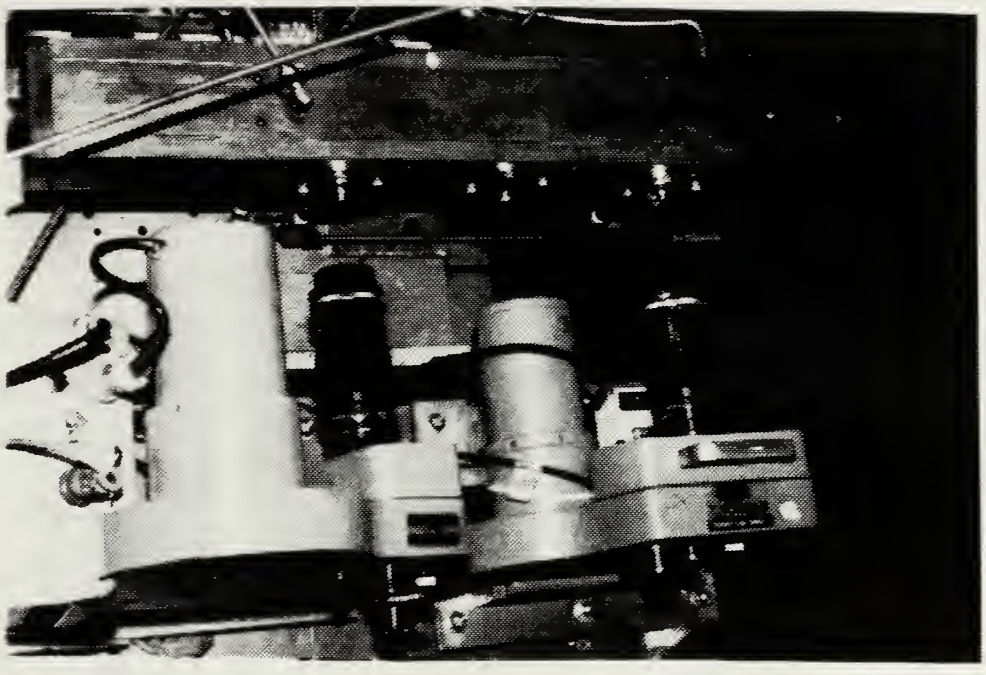

Figure 3.10 Instalation of the Two HYCAM Cameras.

TABLE 4
DEPTH OF FIELD VS. F STOP

f stop	Depth of Field (mm)
3	± 3.7
5.6	± 5.7
8	± 7.2
11	± 8.9
16	± 10.6
22	± 11.7

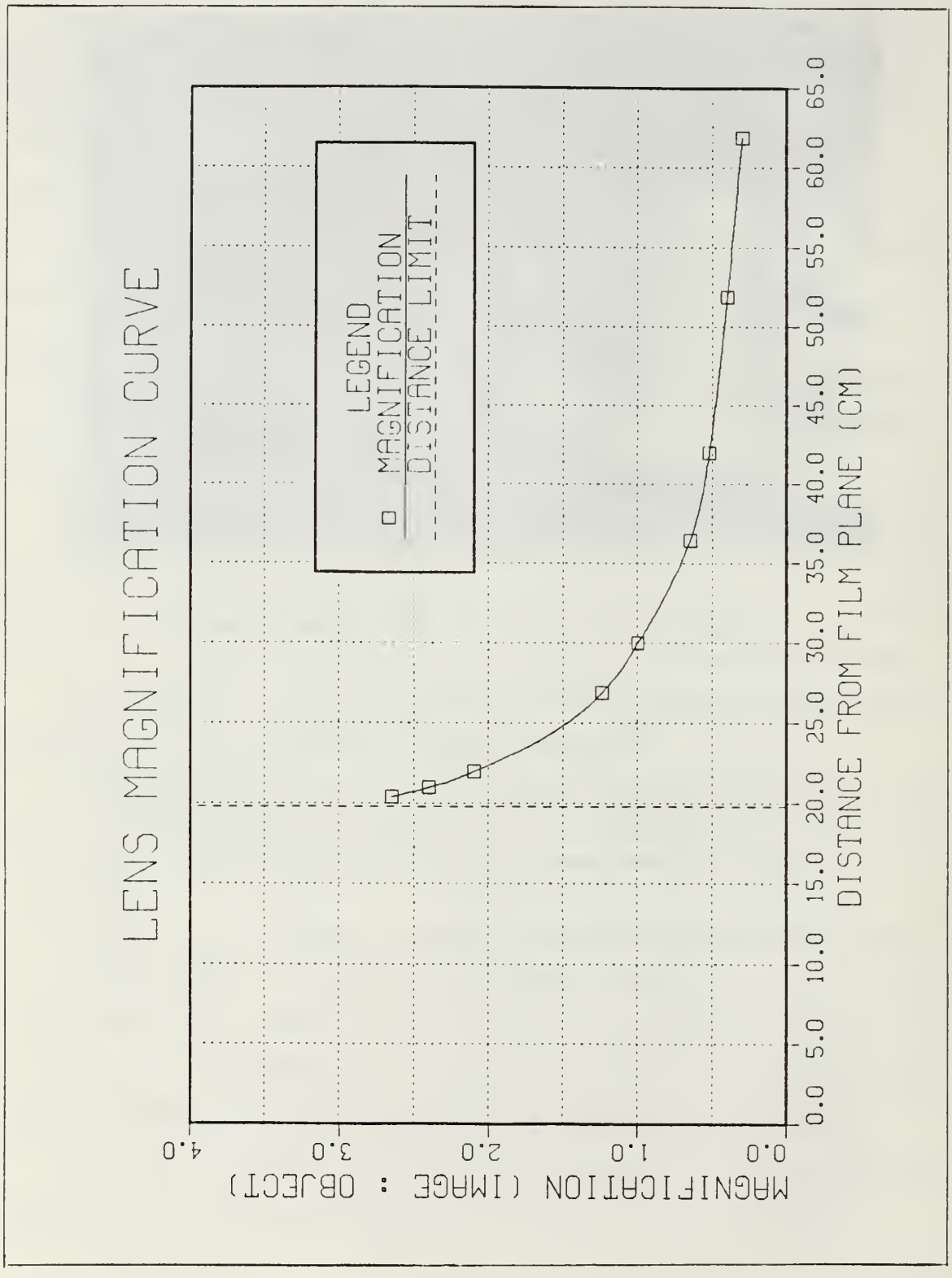

Figure 3.11 Magnification vs. Distance from Subject.

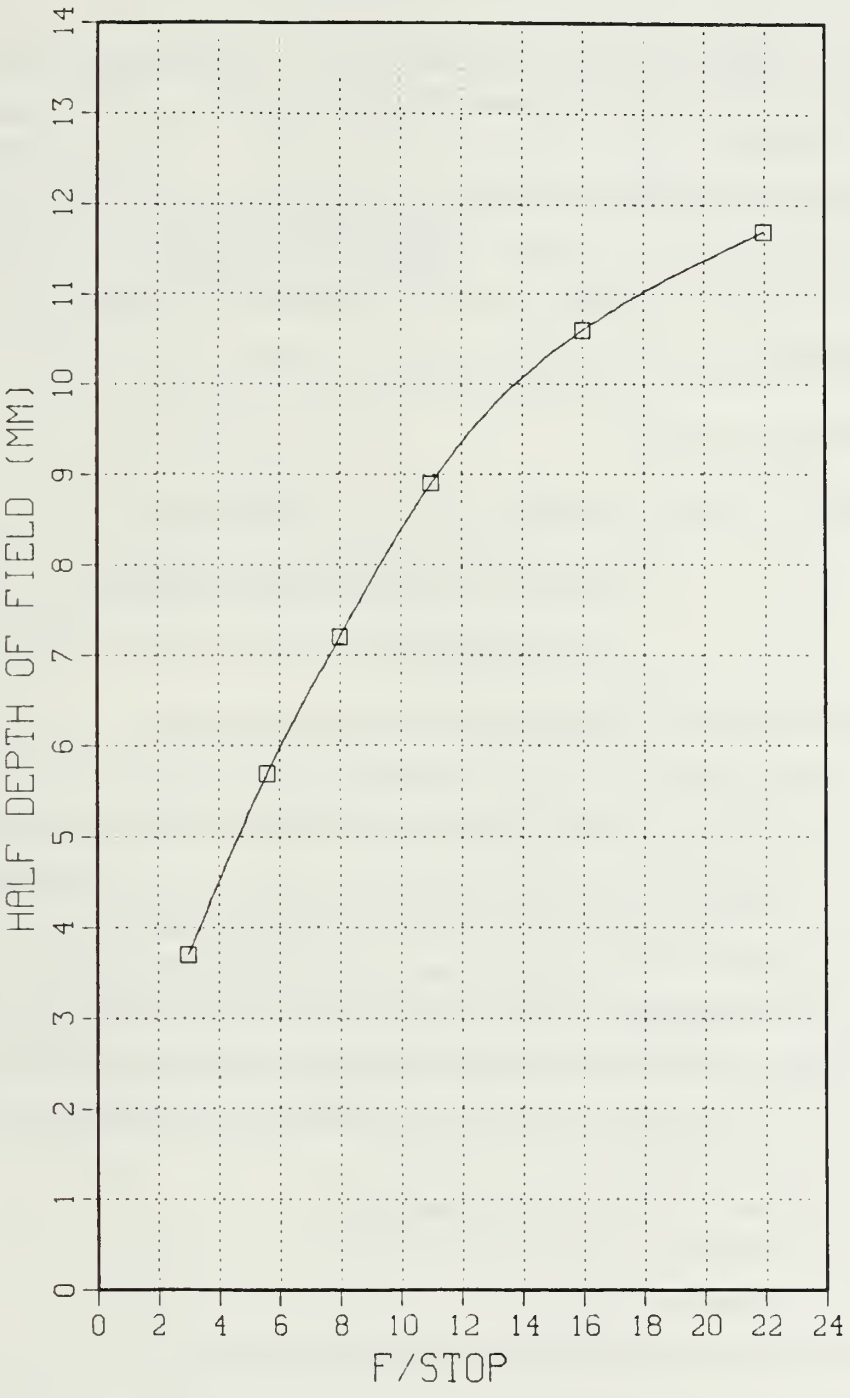

Figure 3.12 Depth of Field vs. f/stop for 1:1 Magnification.

IV. EXPERIMENTAL METHOD

Nine different solid metallized fuels were investigated (see table 5). They were provided by the Naval Weapons Center (NWC) and the Atlantic Recearch Corporation (ARC).

The fuel compositions had varying amounts of B_4C, Mg, polytetrafluoroethylene, zirconium and binder. The metal contents were typically between 50% and 70% by weight. In Table 5 the composition order is given in the following sequence: [2]

B_4C/Mg/polytetrafluoroethylene/Zr/binder.

The reference condition is:

B_4C/Mg/poly/Zr/binder (equal parts B_4C and Mg. Minimum quantities or no polytetrafluoroethylene and zirconium).

The solid fuel was placed on the bottom and on the top sides of the two-dimensional motor in order to make it possible to take pictures of the interior of the SFRJ motor during the combustion process. It was in the form of slabs 16 inches long and 2.5 inches wide. The thickness was 0.25 inches. Because of the fact that only limited quantities of metallized fuels were available, only the bottom side was covered with metallized solid fuel. It was 16 inches long and the width was usually 1 or 1.5 inches. The rest of the bottom side was filled with zecorez or HTPB solid fuels. The top side was covered also with zecorez or HTPB. Pictures of the surface or of the space close to the surface of the metallized solid fuel were taken at the reattachment point and just prior to the mixing chamber.

Two air mass fluxes (G) were investigated:

a. $G \sim 0.2$ lbm/sec-in^2 (Low G)
b. $G \sim 0.5$ lbm/sec-in^2 (High G)

These mass fluxes corresponded to air mass flow rates of 0.5 and 1.25 lbm/sec.

---

[2]An exception to this nomenclature was the fuel supplied by ARC.

TABLE 5
METALLIZED FUELS

FUEL TYPE	PROVIDED BY	REFFER. NUMBER
B_4C/Mg/poly/Zr/binder (equal parts B_4C and Mg. Minimum quantities or no polytetrafluoroethylene and zirconium). (Refference condition).	NWC	1
B_4C + 10%/Mg-10%/poly/Zr/binder	-"-	2
B_4C + 15%/Mg-20%/poly/Zr/binder + 5%	-"-	3
B_4C/Mg-2%/poly/Zr + 2%/binder	-"-	4
B_4C/Mg-5%/poly/Zr + 5%/binder	-"-	5
B_4C + 15%/Mg-30%/poly + 5%/Zr/binder + 10%	-"-	6
B_4C + 5%/Mg-20%/poly + 5%/Zr/binder + 10%	-"-	7
B_4C + 15%/Mg-35%/poly + 10%/Zr/binder + 10%	-"-	8
B/Teflon	ARC	9

For each air mass flux, a test was attempted for each fuel under a high and a low combustion pressure.

The inlet air temperatures were between 993 and 1234 °Rankine.

The inlet height was 0.35 in. [3]

The motion pictures were observed using a stop action projector to examine the surface and adjacent gas flow combustion phenomena and also to analyze the size, trajectories and velocities of the particles.

[3]For the experiment NWC-24 the inlet height was 0.5 in.

V. RESULTS AND DISCUSSION

A. MOTOR OPERATION

In general a two-dimentional SFRJ combustor is more difficult to operate than an axisymmetrical one because of the heat loss to the side walls and the lack of sufficient gaseous fuel and heat generation within the recirculation zone. In almost all of the high G and in some of the low G experiments, especially with low combustion pressures, it was difficult to sustain the combustion process after the ignitor was shut off, even with the inlet step blocks that provided the small inlet area (0.35 in × 2.5 in). This problem was corrected in some of the low G tests by using a smaller nozzle throat diameter in order to obtain a higher combustor pressure (P_c). [4] Motor inlet air temperatures higher than 1264 °R were not attempted in order to protect the system from damage due to high temperature. [5]

When the inlet step height (h) was too small (fuel thickness more than 0.25 inches and/or inlet height equal to 0.5 inches) it was often imposible to stabilize the flame. However, the value of Ap/Ai could not be increased more than about $(1 \times 2.5)/(0.35 \times 2.5) = 2.86$ with existing hardware and the fuel slabs could not be thiner than 0.25 inches. Smaller inlet areas would have resulted in excessive inlet velocities.

During practically all of this investigation the two-dimentional motor was operated with uninsulated side-walls and with a five-second air pre-heat time before ignition. These conditions resulted in ignition difficulties at all pressures with high G and at low pressures with low G. At the conclusion of the investigation a solution to this problem was found. One side wall (opposite to the window ports) was insulated with black Plexiglas and the air pre-heat time was increased to ten seconds. These modifications resulted in succesful tests at high G with both high and low pressures.

Appendix B shows the conditions under which the solid metallized fuels were tested and the ability of the fuel to ignite and sustain under those conditions.

---

[4]The combustion pressures ranged between 57 and 185 psia.

[5]The average motor inlet air temperature was 1088 °R

Initially, problems were encountered with the two viewing windows. The nitrogen used as the window purge gas was quenching the combustion process, so compressed air was substituted for nitrogen as the window purge gas. Use of the compressed air helped, but the problem did not disappear at the front viewing window. With high window purge air mass flow rate at the front viewing window, the combustion process was quenched and with lower mass flow rate the window was fowled and burned. In order to solve this problem, after the first six experiments, the 1.5 inches diameter sintered ring between the Plexiglas window and the steel plug was replaced with a steel ring with six drilled holes to allow the flow of air through them. Another sintered ring of a smaller diameter (0.3 inches) was placed between the Plexiglas and the 0.5 inch drilled hole of the steel plug. This design proved quite acceptable from the stand point of ignitability of the fuel and cleanliness of the viewing windows.

Appendix B shows the test conditions and the ignition behavior of each fuel tested. Tables 6 and 7 show how the pressure affected the ignitability of the fuels for both high and low mass fluxes. Appendix C gives a summary of what has been observed in the films. Films were not obtained for all the experiments for one or more of the following reasons: (1) Sometimes only the top-side fuel ignited, (2) With the old window purge system, the windows almost always burned before the pictures could be taken, (3) Sometimes the solid fuel would not sustain more than a few seconds, and (4) Sometimes the films were taken after shutdown.

B. SUMMARY OF TEST RESULTS AND MAJOR OBSERVATIONS FROM FILMS

A more detailed description of the combustion characteristics of each fuel for different test conditions is given below. The flow in the pictures is from right to left and the scale is approximately 11:1.

In the films discussed below, some common characteristics were observed. When glowing white particles were observed, they were assumed to be ignited particles. Particles which were orange in color (much like the surface of many of the fuels) were assumed to be hot, but unignited. These assumptions are based upon present and past observations in which particles sometimes are observed leaving the surface with an orange color and then, after passing into the oxygen containing gases well above the surface, ignite into a white glowing particle. Also observed in most of the films was a shedding or ejection of dark, unignited small flakes of material. Since they were

TABLE 6

EFFECT OF PRESSURE ON IGNITION CHARACTERISTICS AT LOW G

FUEL #	NO IGNIT.	IGNIT./NO SUST.		SUSTAIN	
TABLE 5	AIR ONLY PRESSURE (psia)	AIR ONLY PRESSURE (psia)	IGNIT. PRESSURE (psia)	AIR ONLY PRESSURE (psia)	SUST. PRESSURE (psia)
4	30	44/45	80/67	43	100
5		33	69	72/51	148/86
1				52/53	74/84
2	33			78/41	150/75
3		32/46	65/71	62/91	140/183
6		36/45	59/77	73	156
7		37	57	75	152
8		29/51	65/83	70	148
9		27	62	70/50	149/95

observed for fuels of widely different metallic content it was presumed (although not known)that they were binder material. Larger flakes/layers were observed which contained hot particles.

In earlier studies it has been observed that when particles ignite, their apparent diameter increases by approximately a factor of four. If this remained the case in the present study, then typical observed particle sizes (within the flame envelope) were between 10 and 175 μm, with an occasional very large particle of approximately 750 μm. Smaller particles may have been present, but were beyond the resolution limits of the motion pictures.

1. **B_4C/Mg/polytetrafluoroethylene/Zr/binder**

This solid fuel was tested only for low G and low combustion pressures. Two experiments were done (NWC-6 and NWC-7), with combustion pressures equal to 74 and 84 psia respectively. The first time (NWC-6) the fuel ignited and sustained but films were not obtained because the windows were (quickly) burned (old window purge system). The second time (NWC-7) the experiment was done under the same conditions, and the new window purge system was used which insured clean viewing

TABLE 7

EFFECT OF PRESSURE ON IGNITION CHARACTERISTICS AT HIGH G

FUEL #	NO IGNIT.	IGNIT./NO SUST.		SUSTAIN	
TABLE 5	AIR ONLY PRESSURE (psia)	AIR ONLY PRESSURE (psia)	IGNIT. PRESSURE (psia)	AIR ONLY PRESSURE (psia)	SUST. PRESSURE (psia)
4	48	46/61	76/91	72	138
5				95/49	200/73
1					
2					
3					
6		105	185		
7	47	98/41	190/94	90	173
8					
9		88	180		

windows. However, the films did not show anything because the metallized fuel was not burning during the time the pictures were taken.

2. **B_4C + 10%/Mg-10%/polytetrafluoroethylene/Zr/binder**

Three experiments were conducted with this solid fuel, for low G and both high and low combustion pressures.

In the first experiment (NWC-8) the combustion pressure was about 153 psia. The fuel ignited and sustained very well under these conditions. Films were obtained for both the recirculation zone and the boundary layer region. In the recirculation zone the fuel surface was glowing. Surface agglomerates were not observed. Many individual glowing metal particles were coming out of the fuel surface. They were of two kinds: small ignited (white) particles (see Figure 5.1) with an average diameter equal to 0.6 mm, and larger unignited (yellow/orange) particles with a maximum diameter observed equal to about 1.5 mm. A lot of thin surface flakes were observed that did not ignite when they entered the gas phase zone (see Figure 5.2). Their size was apporximately 0.10 × 0.10 mm. Once-in-a-while large flakes were ejected from the fuel surface. The largest flake observed had dimentions 1.0 mm × 1.5 mm × 0.2 mm

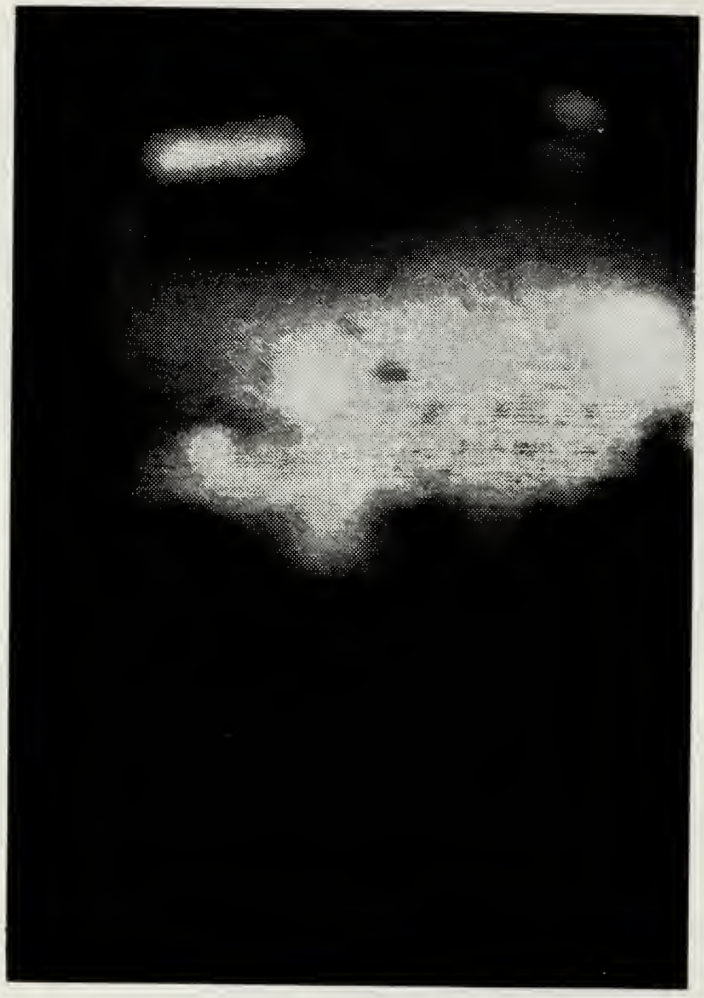

Figure 5.1 NWC-8/Recirculation Zone/Low G/High P_c.

thick. When they left the fuel surface they would disintegrate and form smaller non-burning flakes. The film taken in the boundary layer region showed a lot of small, and some large, burning white particles in the gas phase region. Some yellow particles were stuck on the surface or were rolling on it. Sometimes they ignited to become white. Medium and large sized flakes were occasionally observed coming from the surface.

In the second experiment (NWC-9) the conditions were the same as the previous one (NWC-8), but the lenses were focused on a point closer to the viewing window. The surface was tapered at the focusing point and a larger apperture was used (5.6) in order to see how the apperture effected the quality of the pictures. [6] In this run the fuel ignited and sustained easily with a combustion pressure equal to about 150 psia.

---

[6]Comparison of the pictures showed that f/stop 11 gave better pictures than 8 and 5.6 for 6000 PPS. However f/stop larger than 11 has not been tested.

Figure 5.2 NWC-8/Recirculation Zone/Low G/High P_c.

In the third experiment (NWC-10), a low pressure run was attempted. With an air-only pressure equal to about 32 psia the fuel did not ignite. With an air-only pressure of about 41 psia it ignited and sustained an average pressure equal to 75 psia. During the pictures the metallized fuel was not burning and so the films did not show anything.

3. **B_4C + 15%/Mg-20%/polytetrafluoroethylene/Zr/binder + 5%**

Three experiments were conducted with this fuel for low G, with combustion pressures equal to 140 psia (NWC-11), 183 psia (NWC-13), and 71 psia (NWC-12).

In the first experiment the fuel ignited easily at an air-only pressure of about 62 psia and sustained a steady state pressure of 140 psia. In the recirculation zone a lot of small ignited (white) and unignited (glowing, orange) particles were observed.

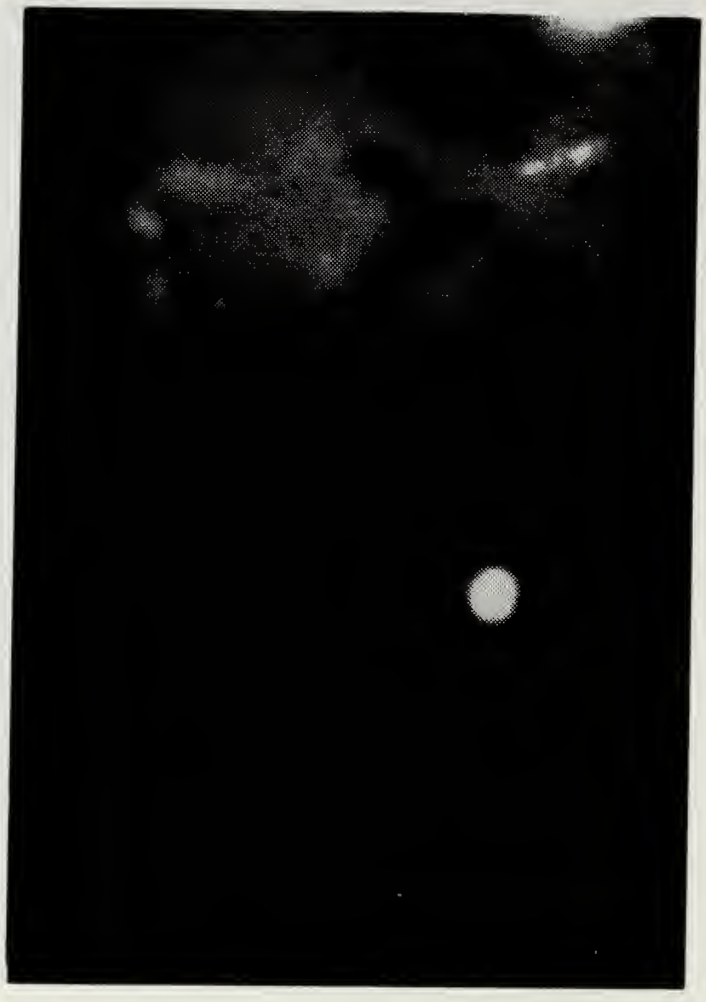

Figure 5.3 NWC-11/Recirculation Zone/Low G/High P_c.

Compared with the B_4C+10%/Mg-10%/polytetrafluoroethylene/Zr/binder, more particles were observed but with smaller sizes (on the average 0.18 to 0.40 mm). More tiny surface flakes were also observed. Once-in-a-while some large flakes came off of the surface. A large agglomerate was observed close to the viewing window. It was glowing, and once-in-a-while ignited metal particles were emitted as shown in Figure 5.3. In the boundary layer region the main characteristic was a lot of medium sized ignited (white) particles in the gas phase. Their diameters were between 0.12 and 0.25 mm. Many very small ignited particles were also observed in the gas phase. Their diameters were about 0.05 mm. The burning particles were following low trajectories, sometimes in contact with the fuel surface. Figure 5.4 is characteristic of the boundary layer region behavior. Surface agglomerates were not observed. Occasionally some small, nearly circular flakes left the surface and remained unignited. The largest of them had a diameter equal to 0.5 mm.

Figure 5.4 NWC-11/Boundary Layer/Low G/High P_c.

The second experiment (NWC-12) was at low G and low pressure. With combustion pressure equal to about 65 psia the fuel ignited easily but it would not sustain. With an average combustion pressure equal to 71 psia only the HTPB was burning. The pictures were taken when the metallized fuel was not burning, and so information was not obtained about the characteristics at the low G, low pressure conditions.

The third experiment (NWC-13) was made with low G and high pressure because it was believed that during the NWC-11 experiment the pictures had been taken after the purging of the fuel, and also because metal particles had not been observed in the exhaust flow. During this experiment (NWC-13) the metallized fuel ignited quickly at a pressure equal to about 183 psia. The film in the boundary layer region showed a few ignited (white) particles and a lot of large flakes.

4. **B_4C/Mg-2%/polytetrafluoroethylene/Zr + 2%/binder**

This fuel was tested with high and low G conditions, at both high and low combustion pressure.

The first time (NWC-1) it was tested at high G and different pressures. For an air-only $P_c = 48$ psia the fuel did not ignite. For $P_c = 138$ psia it ignited and sustained. Film was not obtained of the recirculation zone because the window was

burned. In tha boundary layer region the film showed many high speed small particles (diameter ~ 0.1-0.45 mm). A few larger white/yellow ignited particles (1.6-3 mm) were observed close to the fuel surface and in the gas phase. Some medium sized flakes were observed at the end of the film (probably during the shutdown).

With high G and low pressure (76 psia) it barely sustained. Pictures were not obtained because the viewing windows were burned. When the combustion pressure was raised slightly (91 psia) the fuel ignited easily but it did not sustain more than 1.0 second (NWC-3).

For low G and high pressure (100 psia) the fuel ignited and sustained (NWC-4) but the pictures were taken after the purging of the fuel. For low G and low pressure (67 psia) the fuel ignited easily but it did not sustain for more than 2.0 seconds (NWC-5). Film was obtained only in the recirculation zone. It was taken during the shutdown. A lot of small white and pink colored particles were observed.

5. **B_4C/Mg-5%/polytetrafluoroethylene/Zr + 5%/binder**

This fuel was tested at high and low G conditions, and each time with high and low combustion pressure.

For low G and high combustion pressure (148 psia) the fuel ignited easily and sustained (NWC-14). The film in the recirculation zone showed many small (0.1 mm) and large (0.5 mm) ignited particles (see Figure 5.5). Flakes were observed during shutdown with glowing particles embedded in them (see Figure 5.6). In the boundary layer region many small (0.1 mm), and periodically some larger, ignited particles were observed in the gas phase. Periodic shedding of large flakes occurred. Large agglomerates were created on areas where the fuel surface was not smooth (see Figures 5.7 and 5.8). These large agglomerates existed for awhile and then left the surface together with unignited surface material (see Figures 5.9 and 5.10). Near the motor shutdown, more small particles were observed.

For low G and low combustion pressure (NWC-15) the fuel ignited. It would not sustain for $P_c = 69$ psia but sustained for $P_c = 86$ psia. The pictures were taken during the shutdown. In the recirculation zone and in the boundary layer region many very small particles were observed (0.04 mm) and some larger ones (0.7 mm) were observed in the gas phase.

The high G and high pressure experiment (NWC-26) was conducted with the vertical side of the motor opposite to the viewing windows insulated with black Plexiglas. Also, the motor was preheated with the hot inlet air for about 10 seconds

Figure 5.5 NWC-14/Recirculation Zone/Low G/High P_c.

before the ignition (vs 5 seconds on earlier tests).This technique reduced the heat losses and resulted in good ignition and good burning. The measurement of the combustion pressure was lost during this test but was estimated to be about 200 psia. The developed films have not been received to date.

For high G and low pressure (NWC-27) the above technique was used and the ignition and sustained burn were very good. The films have not been received to date.

6. **B_4C + 15%/Mg-30%/polytetrafluoroethylene + 5%/Zr/binder + 10%**

This fuel was tested at high and low G.

For low G and high pressure (156 psia) it ignited easily and sustained (NWC-16). In the recirculation zone not too many ignited (white) particles were observed. A lot of small flakes and some larger ones (0.5 mm × 1.4 mm) were observed leaving the surface. At shutdown, big flakes with ignited particles on them left the

Figure 5.6 NWC-14/Recirculation Zone/Low G/High P_c.

surface (see Figure 5.11). In the boundary layer region not many ignited particles were observed. Flakes left the surface occasionally. Surface irregularities created several large surface agglomerates with shedding particles, and after awhile they left the surface on top of a large flake.

For low G and low pressure (59 psia) the fuel ignited but would not sustain (NWC-17). During the pictures only the HTPB (top side) was burning.

For high G and high pressure (185 psia) the fuel ignited, but would not sustain (NWC-23). The pictures were taken after burnout.

7. **B_4C + 5%/Mg-20%/polytetrafluoroethylene + 5%/Zr/binder + 10%**

This fuel was also tested at low and high G.

For low G and high pressure (152 psia), it ignited and sustained (NWC-19). In the recirculation zone the film revealed ignited particles in the gas phase and on the

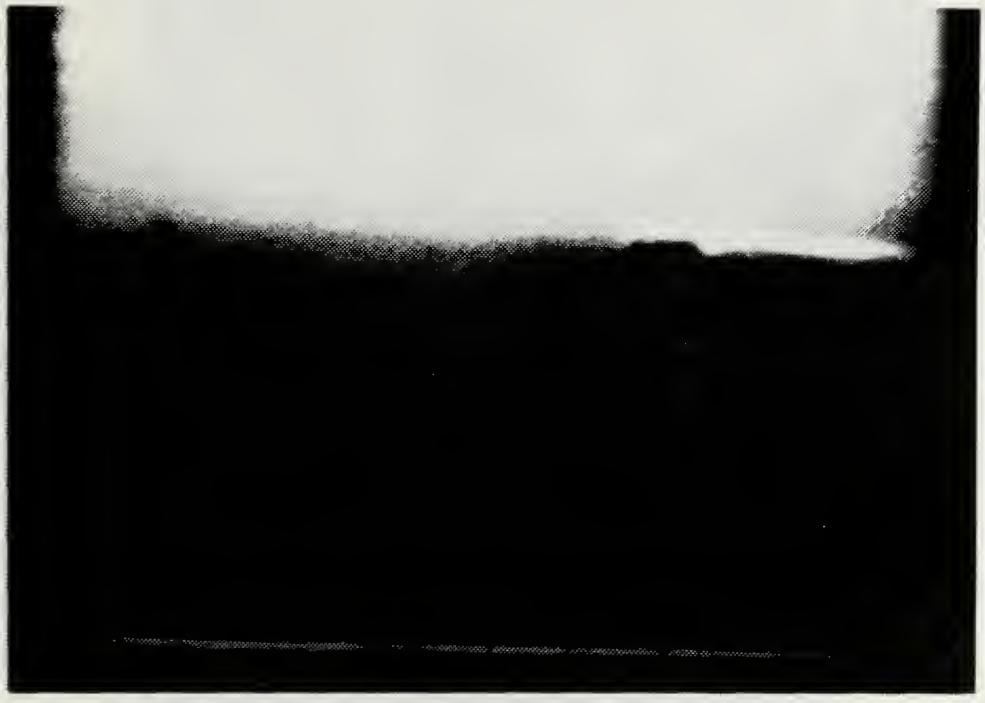

Figure 5.7 NWC-14/Boundary Layer/Low G/High P_c.

Figure 5.8 NWC-14/Boundary Layer/Low G/High P_c.

Figure 5.9 NWC-14/Boundary Layer/Low G/High p_c.

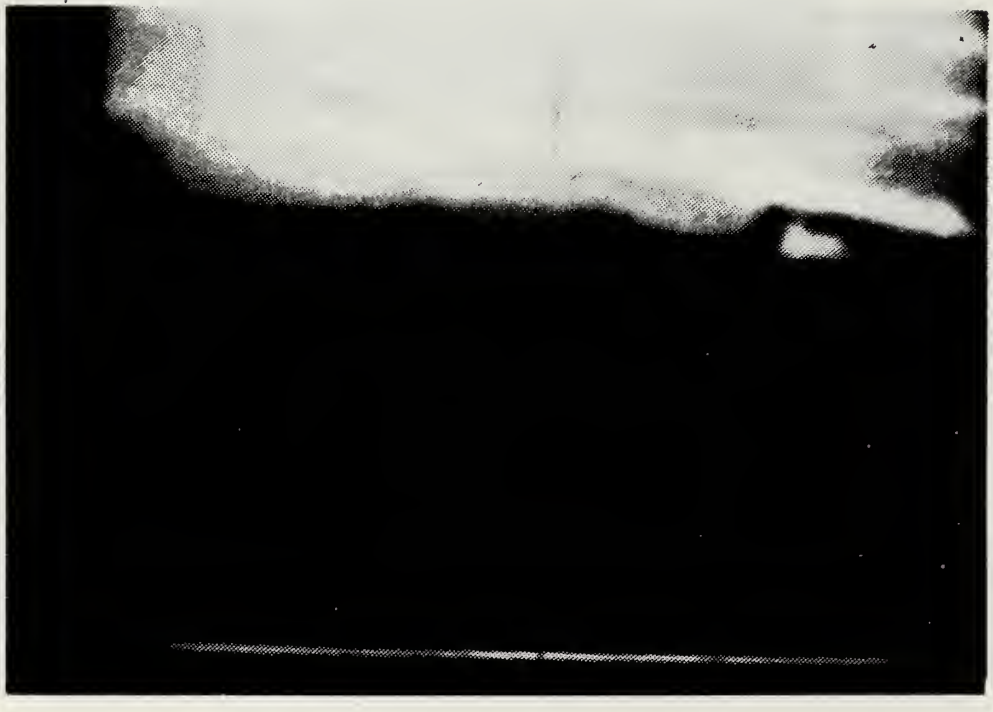

Figure 5.10 NWC-14/Boundary Layer/Low G/High P_c.

Figure 5.11 NWC-16/Recirculation Zone/Low G/High P_c.

surface (see Figure 5.12), and a lot of small and large flakes. Figures 5.13, 5.14 and 5.15 show the sequence of generation of a large flake. The picture of Figure 5.14 was taken 0.33 msec after the picture of Figure 5.13 and the picture of Figure 5.15 was taken 0.66 msec after the picture of Figure 5.14. Characteristics on this flake were that it was large and flat, and had ignited particles embedded in it. At the boundary layer region a lot of small and moderate size flakes were observed leaving the surface. Many small and medium sized particles were also observed in the gas phase. Several large surface agglomerates were created, which after awhile left the fuel surface on top of large flakes. It was characteristic that the upper edge of these agglomerates sometimes ignited (see Figure 5.16).

For low G and low pressure (57 psia) it ignited and barely sustained. During the pictures the metallized fuel was not burning (NWC-20).

Figure 5.12 NWC-19/Recirculation Zone/Low G/High P_c.

For high G and high pressure (190 psia) it ignited and did not sustain, but when the inlet height was reduced (heigher inlet step) it ignited (P_c = 173 psia) and barely sustained (NWC-24). The film was taken after the shutdown. For high G and low pressure (47 psia) it did not ignite. When the combustion pressure was increased to 98 psia it ignited but would not sustain.

8. **B_4C + 15%/Mg-35%/polytetrafluoroethylene + 10%/Zr/binder + 10%**

With this fuel only low G tests were conducted.

For high pressure (148 psia), the fuel ignited and sustained even though the top torch of the motor had not worked (NWC-21). In the recirculation zone there was an absence of ignited particles, probably because of the elimination of most of the magnesium in the fuel. A lot of small flakes were observed leaving the surface continuously (see Figure 5.17). In the boundary layer region no flakes or burning particles were observed.

Figure 5.13 NWC-19, Recirculation Zone, Low G, High P_c.

For low pressure (83 psia), the fuel ignited but did not sustain more than one second.

9. **B/Teflon**

This fuel was tested at low and high G conditions.

At low G and high pressure (149 psia), it ignited and sustained (ARC-2# 1). In the recirculation zone the film revealed a lot of small and large size (7 mm) flat flakes. Burning particles were not observed. However, the presence of a few orange glowing particles in the gas phase and on the surface was noteable. Figures 5.18 and 5.19 show large size flakes in the recirculation zone. Just before shutdown a lot of large flakes left the surface of the solid fuel. In the boundary layer region a lot of medium sized and some large flakes left the surface. Figure 5.20 shows one large sized flake in the gas phase. Burning particles were not observed, probably because of the absence of magnesium.

Figure 5.14 NWC-19/Recirculation Zone/Low G/High P_c.

For low G and low pressure (64 psia), the ignition was difficult and it would not sustain. By increasing the combustion pressure to 95 psia the fuel ignited easily and sustained. In the recirculation zone the film was similar to the one obtained for low G and higher pressure (149 psia). In the boundary layer region many more and larger flakes were observed at this pressure. Surface agglomerates left the surface on top of flakes. Burning particles were not observed.

For high G and high pressure the fuel just ignited but could not sustain, even with very high combustion pressure.

Figure 5.15 NWC-19/Recirculation Zone/Low G/High P_c.

Figure 5.16 NWC-19/Boundary Layer/Low G/High P_c.

Figure 5.17 NWC-21/Recirculation Zone/Low G/High P_c.

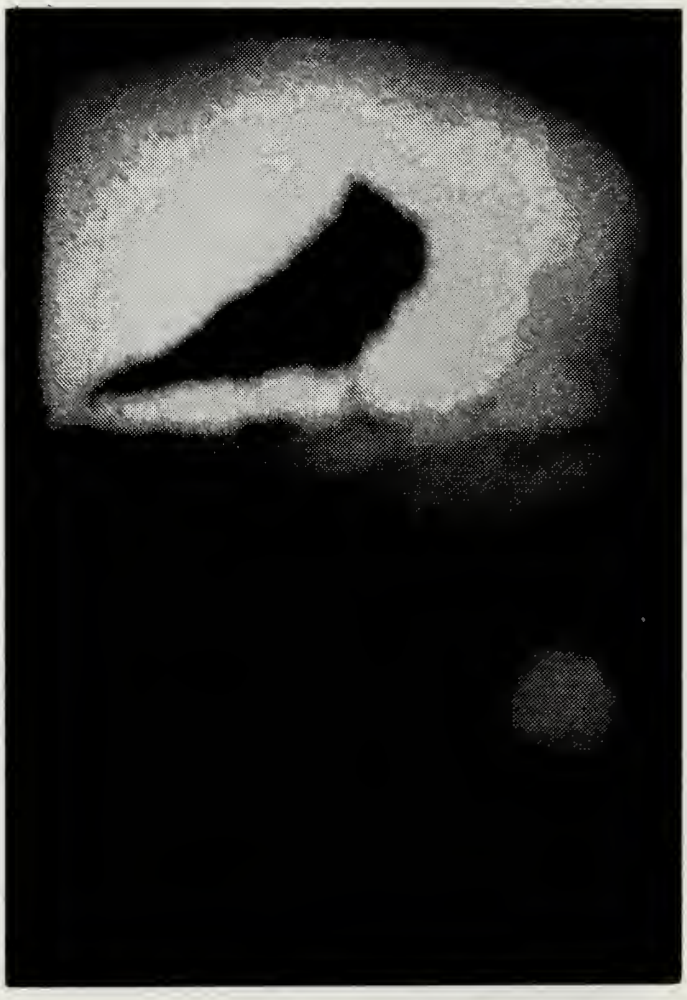

Figure 5.18 ARC-2#1/Recirculation Zone/Low G/Low P_c.

Figure 5.19 ARC-2#1/Recirculation Zone/Low G/Low P_c.

Figure 5.20 ARC-2#2/Boundary Layer/Low G/High P_c.

VI. CONCLUSIONS AND RECOMMENDATIONS

Due to ignition difficulties at high G, most of the tests were conducted for low G conditions, and therefore, enough information was not available to describe accurately the effect of inlet air mass flux on the combustion characteristics of the solid metallized fuels. However, the results of the experiments showed that the higher air mass flux conditions result in poorer ignition characteristics. Insulating one side-wall and increasing the air pre-heat time were found to significantly improve ignition characteristics.

The combustion pressure was one of the most important factors that effected the ignitability of the solid metallized fuels. For higher pressures the fuels ignited and sustained more easily. Also the combusion characteristics of the metallized fuels were effected by the combustion pressure. For lower pressures, the amount and size of the flakes ejected from the surface were larger than for higher pressures.

All the fuels tested exibited a low pressure ignitability limit which was fairly high, due to the heat losses of the two dimentional SFRJ motor. The experiments for low combustion pressure should be repeated with the SFRJ motor insulated and preheated before the ignition.

The effect of composition was probably most important in this metallized solid fuels combustion study. For the fuels tested, it was obvious that the ignited metal particles were related directly to the existence of magnesium in the fuel. When magnesium was not contained in the fuel there were no ignited metal particles in the gas phase or on the fuel surface. This may have been the result of the existence of very small particles (< 10 μm)which were beyond the resolution limits of the motion pictures. Also, the number of ignited particles was proportional to the amount of magnesium contained in the fuel.

The relative amounts of B_4C and Mg in the fuel effected the size of the particles. Increasing the B_4C and decreasing the Mg resulted in smaller particles and more surface flaking.

The existence of Zr in the fuel also effected the surface flaking. With small amounts of Zr in the fuel, flakes were not observed. Those fuels with no Zr or with increased quantities exhibited surface flaking. More data are required to clarify this observation.

The existance of polytetrafluoroethylene resulted in more hot particles on the fuel surface.

During motor shutdown large surface layers were ejected (often containing hot particles), possibly due to thermal gradients or trapped gas. Also during shutdown more ignited particles have been observed, probably due to recirculation. These observations help explain a behavior observed during actual motor firings. Often the ratio of thrust to chamber pressure remains constant during the test, indicating a nearly constant exhaust nozzle throat area. However, post-fire examination of the nozzle normally shows the existence of significant deposits which reduce throat area. Apparently, these deposits are made only during the shutdown proces.

APPENDIX A

SAMPLE COMPUTER PRINTOUT

**** PRE-RUN INPUT ****

Testno=	NWC-11	Date=	11-12-86	Fuelid$=	50/15	Pbar=	14.70		
Heaterfuel=	METHANE	Ignitionfuel=	ETHYLENE	Purge gas=	NITROGEN				
Wtfi=	99.0000	Dp=	1.130	Lp=	16.000				
Di=	.350	Dth=	.750						
Tma=	25.0	Tmi=	0.0	Tmb=	0.0	Tmp=	0.0		
Dairchoke=	.235	Dhtfuchoke=	.025						
Dhtoxchoke=	.067	Dighfuchoke=	.038						
Dpurgechoke=	.220								
Cdair=	.970	Cdh=	.970	Cdho=	.970				
Cdp=	.970	Cdif=	.970						
Gammahf=	1.320	Gammaif=	1.220						
Gammap=	1.400								
Rhf=	96.40	Rif=	55.10	Rp=	55.16				
Kmhf=	.3876	Kmif=	.4985	Kmp=	.5229				
Kmho=	.5589	Kmair=	.3320						
Maird=	.500	Tid=	0.0						
Mhfd=	.0055	Mhod=	.0220	Mifd=	.0033	Mod=	.4000		

**** DATA EXTRACTED ****

FLOW RATES IN Lbm/sec, PRESSURE IN Psia, TEMPERATURE IN R

Time(sec)	Mair	Mhf	Mho	Mif	Ti	F(Lbf)	Pc	Ph	Ta
.50	.470	.0063	.0241	0.0000	601.3	0.0	30.1	130.7	505.0
1.00	.470	.0062	.0244	0.0000	708.9	0.0	53.3	184.7	503.6
1.50	.471	.0063	.0244	0.0000	789.7	0.0	57.3	191.8	505.5
2.00	.470	.0062	.0248	0.0000	843.3	0.0	59.4	203.4	501.4
2.50	.471	.0063	.0247	0.0000	888.9	0.0	61.0	199.2	504.5
3.00	.471	.0063	.0250	0.0000	920.4	0.0	61.5	194.7	503.6
3.50	.470	.0063	.0251	0.0000	945.3	0.0	60.1	196.3	503.2
4.00	.470	.0063	.0250	0.0000	966.3	0.0	63.3	204.3	505.0
4.50	.471	.0063	.0250	0.0000	983.1	0.0	62.4	202.1	503.5
5.00	.471	.0063	.0250	0.0000	997.6	0.0	62.1	203.1	503.6
5.50	.471	.0063	.0275	.0033	1005.4	0.0	64.1	203.4	502.7
6.00	.471	.0063	.0246	.0026	1017.6	0.0	73.2	208.0	505.9
6.50	.472	.0063	.0253	.0029	1024.6	0.0	118.2	283.0	503.2
7.00	.471	.0062	.0257	.0030	1031.2	0.0	137.3	286.3	500.9
7.50	.471	.0063	.0252	.0028	1043.0	0.0	142.2	214.3	505.5
8.00	.472	.0063	.0258	0.0000	1048.2	0.0	141.0	212.4	505.5
8.50	.471	.0063	.0259	0.0000	1052.1	0.0	139.8	212.4	503.6
9.00	.471	.0063	.0255	0.0000	1058.7	0.0	139.7	215.1	505.5
9.50	.472	.0063	.0258	0.0000	1063.4	0.0	141.6	218.8	503.6
10.00	.472	.0063	.0255	0.0000	1039.9	0.0	87.1	252.8	502.3
10.50	.470	.0063	.0249	0.0000	991.4	0.0	19.8	51.0	508.2
11.00	.472	.0063	.0256	0.0000	955.1	0.0	7.4	14.7	500.9
11.50	.472	.0038	.0031	0.0000	950.2	0.0	8.5	14.7	501.8
12.00	.472	.0011	.0004	0.0000	920.4	0.0	7.9	14.7	501.4
12.50	.472	.0009	-.0002	0.0000	912.0	0.0	6.8	14.6	497.7
13.00	.471	.0010	-.0005	0.0000	918.4	0.0	8.2	14.7	503.6
13.50	.471	.0010	-.0005	0.0000	907.1	0.0	7.9	14.7	502.3
14.00	.472	.0009	-.0002	0.0000	899.6	0.0	6.8	14.6	499.5
14.50	.472	.0010	-.0005	0.0000	897.8	0.0	8.5	14.7	502.3

APPENDIX B

SUMMARY OF MOTOR TEST CONDITIONS

TEST NUMBER	FUEL REF. # TABLE 5	D_{th} in	AIR ONLY psia	G_{tot} $\frac{lbm}{s\text{-}in^2}$	P_c IGNIT./SUST. psia	T_i °R	COMMENTS
NWC-1	4	1.35	48	.52	-/-	1180	No ignition
	4	1.12	72	.54	-/138	1180	Difficult ignition and sustain
NWC-2	4	1.35	46	.52	-/76	1264	Difficult ignition. Barely sustains.
NWC-3	4	1.12	61	.53	91/-	1234	Good ignition. No sustain.
NWC-4	4	1.12	30	.22	-/-		No ignition
	4	0.95	43	.20	-/100	1106	Ignition and sustain
NWC-5	4	0.95	45	.20	-/67	1052	Ignition. Hard to sustain.
NWC-6	1	0.95	52	.22	-/74	1050	-"-
NWC-7	1	0.95	53	.22	-/84		Good ignition. Good sustain.
NWC-8	2	0.75	73	.21	-/153	1072	-"-
NWC-9	2	0.75	78	.21	-/150	1075	-"-
NWC-10	2	1.35	29	.21	-/-	1063	No ignition
	2	1.25	20	.20	-/-	1099	-"-
	2	1.12	33	.20	-/-	1117	-"-

TEST NUMBER	FUEL REF. # TABLE 5	D_{th} in	AIR ONLY psia	G_{tot} $\frac{lbm}{s\text{-}in^2}$	P_c IGNIT./SUST. psia	T_i °R	COMMENTS
	2	0.95	41	.20	-/75	1125	Ignition. Hard to sustain.
NWC-11	3	0.75	62	.20	-/140	1055	Good ignition. Good sustain.
NWC-12	3	1.12	32	.20	65/-	1147	Ignition. No sustain.
	3	0.95	46	.20	-/71	1120	Ignition. Hard to sustain.
NWC-13	3	0.75	91	.29	-/183	993	Good ignition. Good sustain.
ARC2#1	9	0.75	70	.21	-/149	1033	-"-
ARC2#2	9	1.12	27	.21	62/-	1125	Difficult ignition. No sustain.
	9	0.95	50	.21	-/95	1064	Good ignition. Good sustain.
NWC-14	5	0.75	72	.21	-/148	1028	Good ignition. Good sustain.
NWC-15	5	1.12	33	.21	69/-	1114	Ignition. No sustain.
	5	0.95	51	.22	-/86	1046	Good ignition. Good sustain.
NWC-16	6	0.75	73	.23	-/156	1076	-"-

TEST NUMBER	FUEL REF. # TABLE 5	D_{th} in	AIR ONLY psia	G_{tot} $\frac{lbm}{s\text{-}in^2}$	P_c IGNIT./SUST. psia	T_i °R	COMMENTS
NWC-17	6	1.12	36	.22	-/59	1082	Ignition. Hard to sustain.
NWc-18	6	0.95	45	.21	-/77	1047	Good ignition. Sustains.
NWC-19	7	0.75	75	.22	-/152	1051	Good ignition. Good sustain.
NWC-20	7	1.12	37	.22	-/57	1125	Good ignition.Barely sustains.
NWC-21	8	0.75	70	.21	-/148	1048	Good ignition. Good sustain.
NWC-22	8	1.12	29	.21	65/-	1040	Ignition. No burn.
	8	0.95	51	.22	83/-	1085	Good ignition. No sustain.
NWC-23	6	0.95	105	.51	185/-	1141	Good ignition. No sustain.
NWC-24	7	0.95	98	.54	190/-	1075	Good ignition. No sustain.
	7	0.95	90	.53	-/173	1125	Good ignition. Barely sustains.
NWC-25	7	1.35	47	.48	-/-	1160	No ignition

TEST NUMBER	FUEL REF. # TABLE 5	D_{th} in	AIR ONLY psia	G_{tot} $\frac{lbm}{s\text{-}in^2}$	P_c IGNIT./SUST. psia	T_i ^oR	COMMENTS
	7	1.25	48	.4	-/-	1105	-"-
	7	1.12	42	.3	80/-	980	Good ignition. No sustain.
ARC2#3	9	0.85	88	.3	180/-	150	Ignition. No sustain.
NWC-26	5	0.95	95	.52	-/200	1000	Good ignition. Good sustain.
NWC-27	5	1.35	49	.53	-/73	1152	-"-

APPENDIX C

SUMMARY OF OBSERVATIONS

TEST	WINDOW A		WINDOW C		COMMENTS ON FILMS A=Recirculation zone C=Boundary layer region
	f-stop	condit.	f-stop	condit.	
NWC-1	8	burned	11	dark	A: No film. C: Poor pictures. Small high speed burning particles. Some larger particles.
NWC-2	8	-"-	11	-"-	A: No film. C: -"-
NWC-3	11	dark	8	clean	A: No film. C: Non burning fuel.
NWC-4	11	-"-	8	dark	A: No film. C: No film.
NWC-5	11	-"-	8	clean	A: Film at burn out. A lot of small white and yellow particles. C: No film (broken).
NWC-6	11	-"-	8	dark	A: No film. C: No film.
NWC-7	11	clean	8	clean	A: No film (Non burning fuel). C: -"-
NWC-8	11	-"-	8	clean	A: Good film. White and orange/yellow particles. Turbulent flow. Unburned flakes come off of the surface. Eruptions

TEST	WINDOW A		WINDOW C		COMMENTS ON FILMS A=Recirculation zone C=Boundary layer region
	f-stop	condit.	f-stop	condit.	
					on the hot surface. C: Many burning white magnesium particles in the gas phase. Glowing particles on the surface and flaked occasionally.
NWC-9	5.6	clean	5.6	clean	A: Not Received to date. C: -"-
NWC-10	5.6	clean/ spots	5.6	-"-	A: No film (Non burning fuel). C: -"-
NWC-11	11	-"-	11	-"-	A: A lot of small glowing and burning particles. A lot of small flakes and some larger ones. Surface agglomerates. C: Many burning medium size particles. Low trajectories, sometimes in contact with the surface. No agglomerates
NWC-12	11	clean	11	-"-	A: No film (Non burning fuel). C: -"-
NWC-13	11	clean/ spots	11	-"-	A: Film not received. C: Not many burning particles. Large surface flakes.
ARC2#1	11	spots	11	-"-	A: A lot of large flakes. Absence of

TEST	WINDOW A		WINDOW C		COMMENTS ON FUELS A=Recirculation zone C=Boundary layer region
	f-stop	condit.	f-stop	condit.	
					burning particles. A few glowing particles. C: Surface flaking. No particles.
ARC2#2	11	spots	11	clean	A: As with ARC2#1. C: More and larger surface flakes than for higher P_c(ARC2#1). No particles.
NWC-14	11	clean	11	-"-	A: Occasional surface flakes. Many small and large particles. Flakes with particles on them during shutdown. Small ignited particles. C: Many small ignited particles in gas phase. Large agglomerates. Periodic flaking.
NWC-15	11	-"-/	11	-"-	A: Many small particles in the gas phase during shut down. C: Film lost.
NWC-16	11	-"-	11	-"-	A: A few ignited particles. A lot of small flakes. Large flakes during shutdown. C: A few ignited particles. Large agglomerates.

TEST	WINDOW A		WINDOW C		COMMENTS ON FUELS A=Recirculation zone C=boundary layer region
	f-stop	condit.	f-stop	condit.	
NWC-17	11	clean	11	clean	A: No film (Non burning fuel). C: -"-
NWC-18	11	-"-	11	-"-	A: -"- C: -"-
NWC-19	11	-"-	11	-"-	A: Ignited particles in the gas phase and on the surface. Small and large flakes. C: Small and moderate size flakes and particles in gas phase. Large surface agglomerates.
NWC-20	11	-"-	11	-"-	A: No film (Non burning fuel) C: -"-
NWC-21	11	-"-	11	-"-	A: A lot of small flakes. Absence of burning particles. C: No flakes. No particles.
NWC-22	11	-"-	11	-"-	A: No film (Non burning fuel). C: -"-
NWC-23			11	clean/ smoke	A: Not used. C: No film (Non burning fuel).
NWC-24			11	clean	A: Not used. C: Film after burnout.
NWC-25					No pictures were taken.

TEST	WINDOW A		WINDOW C		COMMENTS ON FUELS A=Recirculation zone c=Boundary layer region
	f-stop	condit.	f-stop	condit.	
ARC2#3					No pictures were taken.
NWC-26	11	black	11	clean	A: Not received to date. C: -"-
NWC-27	11	clean/ spots	11	-"-	A: -"- C: -"-

LIST OF REFERENCES

1. Zucrow, M. J., *Aircraft and Missile Propulsion, Volume II*, J. Wiley and Sons Inc, New York, 1958.

2. *The Pocket Ramjet Reader*, United Technologies/Chemical Systems Division, 1978.

3. Avery, W. H., *Twenty-Five Years of Ramjet Development, Vol 25, No. 11*, Jet Propulsion, November 1955.

4. Mady, C. J., Hickey, P. J., and Netzer, D. W., *An Investigation of the Combustion Behavior of Solid Fuel Ramjets*, Naval Postgraduate School, CA, September 1977.

5. Netzer, D. W., *Overview of Ramjet and Ducted Rocket Engines for Tactical Missiles*, Naval Postgraduate School, Monterey, CA.

6. Gany, A. and Netzer, D. W., *Fuel Performance Evaluation for the Solid-Fueled Ramjet*, Naval Postgraduate School Report, NPS 67-84-012, October 1984.

7. *Solid Fuel Ramjets*, United Technologies / Chemical Systems Division.

8. Egan, W. J. Jr., *Workshop Report: Potential Solution to Current Flame Stabilization Problems*, 14th JANNAF Combustion Meeting, August 1977.

9. Boaz, L. D. and Netzer, D. W., *An Investigation of the Internal Ballistics of Solid Fuel Ramjets* Naval Postgraduate School, Monterey, CA, March 1973.

10. Metochianakis, M. E., Goodwin, W. V., Katz, U., and Netzer, D. W., *Modeling Solid-Fuel Ramjet Combustion Including Radiation Heat Transfer to the Fuel Surface*, Naval Postgraduate School, Monterey, CA, August 1981.

11. Zucker, R. D., *Fundamentals of Gas Dynamics*, Naval Postgraduate School, Monterey, CA, 1977.

12. Gany, A., and Netzer, D. W., *Combustion Studies of Metallized Fuels for Solid Fuel Ramjets*, Naval Postgraduate School, Monterey, CA.

13. Scott II, C. K., *An Experimental Investigation of Various Metallic / Polymer Fuels in a Two-Dimentional Solid Fuel Ramjet*, M.S. Thesis, Naval Postgraduate School, Monterey, CA, March 1986.

14. Hansen, B. J., *Automatic Control and Data Acquisition System for Combustion Lab Applications*, M.S. Thesis, Naval Postgraduate School, Monterey, CA, October 1982.

15. *HYCAM 16 mm Cameras Operating Manual*, Red Lake Laboratories.

INITIAL DISTRIBUTION LIST

		No. Copies
1.	Defence Technical Information Center Cameron Station Alexandria, Virginia 22304-6145	2
2.	Library, Code 0142 Naval Postgraduate School Monterey, California 93943-5002	2
3.	Department Chairman, Code 67Pl Department of Aeronautics Naval Postgraduate School Monterey, California 93943	1
4.	Professor D. Netzer, Code 67Nt Department of Aeronautics Naval Postgraduate School Monterey, California 93943	2
5.	Professor R. Wood, Code 67Wr Department of Aeronautics Naval Postgraduate School Monterey, California 93943	1
6.	Adonis Karadimitris 34012 - Orei Evia - GREECE	4
7.	Hellenic Navy General Staff TEN B2 Grafeion Ekpaideusews Exwterikou Stratopedon Papagou Holargos Athens - GREECE	4